
MATHEMATICAL MODELLING OF ISSUES IN THE DEPARTMENT FOR EDUCATION

MMATH PROJECT

ADDIE BAKER

*Supervised by Waleed A Ali
Mathematical Sciences Department
In Collaboration with PRiME
University of Bath
2024 - 2025*



ABSTRACT

This project investigates the chronic shortage of secondary school mathematics teachers in England from the nuanced perspective of mathematical modelling, developing and analysing dynamical systems based on the classic SIR framework prevalent throughout epidemiology.

The first system, a three-stage compartmental model - Early Career Teachers (0 – 2 years), Mid-Stage Teachers (2 – 10 years), and Long-Term Teachers (10+ years) - incorporates key dynamics such as recruitment, retention, and the support-driven transition between “Comfortable” and “Vulnerable” states. Numerical investigations, using Python, validate the model’s behaviour, identifying a key threshold for which attrition dominates the system. These observations are further supported by steady state and local stability analyses which yield explicit conditions on recruitment and attrition rates to achieve a sustainable, predominantly comfortable workforce which may be exploited by the Department for Education to meet their hiring targets each year. To enhance our model’s accuracy, we then develop our system of equations beyond fixed parameter values: including time-dependent functions for attrition fit from government census data, a sinusoidal plus linear function for birthrate to account for cyclic hiring patterns, and a support function which synthesises: salary, burnout, CPD, job satisfaction, workload and student misbehaviour.

A brief investigation is then undertaken on a two-state game-theoretic model, analogous to the original SIR model, which includes best-response and imitation dynamics to model how social structures and personal utility functions based on salary, workload, burnout and job market risk, may effect the greater workforce dynamics. Once again carrying out steady state and local stability analyses provides a series of conditions for stability of each steady state, which may be used to inform policymakers and internal support teams within schools to better support their wider workforce based on social influence.

Following this, both models are generalised to careers beyond teaching and an investigative framework is provided for those who wish to repeat the work carried out in this project.

Contents

1	Introduction	5
1.1	The Maths Teacher Crisis in the UK	5
1.2	Aims and Objectives of the Research	6
2	General Model	7
2.1	Description and Motivation	7
2.2	Non-Dimensionalisation	9
2.3	Numerical Investigations	12
2.4	Steady State Analysis	15
2.5	Stability Analysis	18
2.6	Parameter Investigations	22
3	Extended Model	23
3.1	Time-Dependent β_i	24
3.2	Functional Birth Rate $B(t)$	26
3.3	Variable Support $K(\mathbf{x})$	28
4	Opinion Polling in Teacher Recruitment	35
4.1	Game Theoretic Model Description	35
4.2	Incorporating Best-Response Dynamics	37
4.3	Incorporating Imitation Dynamics	38
4.4	Steady State Analysis	39
4.5	Stability Analysis	41
5	Adapting to Careers Beyond Teaching	44

5.1	Career Progression Framework:	45
5.2	Local Decision-Driven Framework	46
6	Conclusions and Future Work	48
6.1	Summary of Findings	48
6.2	Limitations and Assumptions	50
6.3	Policy Implications	51
6.4	Recommendations for Future Research	54
	Appendices	56
A	List of Acronyms	56
B	Section 2.3 Python Code	57

1 Introduction

1.1 The Maths Teacher Crisis in the UK

The recruitment and retention of secondary school mathematics teachers remains a significant challenge for the Department for Education highlighted in a recent report by the National Foundation for Educational Research (NFER, 2024) which shows the UK government's consistent failure to meet their ever-increasing hiring targets, rising this year to over 3,000 ITT (Initial Teacher Training) graduates (Department for Education, 2024a). In 2023/24, only 63% of the target was met for postgraduate ITT recruitment with a forecasted 76% for 2024/25 based on ITT applications made as of February 2024 (NFER, 2024). The government's shortfall has continued to perpetuate class sizes of up to 50 pupils (Department for Education, 2023b) due to a lack of specialist teachers, exacerbating the challenge of providing personalised support to students. Additionally, according to recent government attrition data, almost 20% of newly qualified teachers leave the profession with their first 2 years of their career, rising to a total of 40% within their first 10 years (Department for Education, 2023b). With such high turnover, it is clear that more needs to be done to retain the teaching workforce in order to ensure a high-quality mathematics education for students across the country.

To address the shortage in qualified mathematics teachers, schools throughout England are using teachers from other subjects to supplement the deficit (Mathematics in Education and Industry, 2024) with a recent government census finding 23.4% of secondary mathematics teachers have no relevant qualification post A-Level, and a further 56.6% have no relevant qualification at degree level or higher (Department for Education, 2023b). The charity "Mathematics in Education and Industry" (MEI) further highlights that poor quality teaching from non-specialists could potentially harm the outcome of students; with a significant decrease in recruitment and increase in attrition after the COVID-19 pandemic (NFER, 2024), could this explain the sudden decrease in students achieving a grade C/4 or above in their mathematics GCSE (Ofqual, 2024)?

In an effort to attract more candidates to ITT courses, individuals enrolling on a Mathematics PGCE in the UK are automatically applied for a £29,000 bursary so long as they hold a 2:2 degree classification or higher in their bachelor's degree, or hold a masters or PhD of any classification (Get Into Teaching, 2024). Additionally, the Institute of Mathematics and its Applications (IMA) offer an additional scholarship of £31,000 to applicants holding a 2:1 or higher in their bachelor's degree, or hold a master's or PhD of any classification (Teaching Maths Scholars, 2024). For teachers already working in the profession, a new early career payment scheme introduced by the government in September of 2024 allows secondary school mathematics teachers to receive up to a further £7,500 depending on their constituency (Department for Education, 2024c). Despite this, the NFER reports that although financial incentives help to drive recruitment in shortage subjects (these being maths, physics, computing and modern foreign languages), they appear to not have any meaningful impact on retention, giving rise to a "take the money and run" mentality (NFER, 2024). More generally however, the teaching profession struggles to compete with the salaries offered by other career paths for STEM graduates, offering little

career progression compared to roles in business, finance and industry (NASUWT, 2019).

Across the literature, and more widely the UK as a whole, it is acknowledged that the UK teaching profession is in crisis; with teacher to student ratios falling each year (Department for Education, 2023b) something needs to be done to address this rising concern.

1.2 Aims and Objectives of the Research

There is currently a significant gap in the literature surrounding the teacher crisis from a mathematical modelling and dynamical systems approach. This project aims to use these tools to investigate issues within and around the workforce management. Current literature focuses its attention on psychological and pedagogical perspectives (Chang, 2009) that put pressure on already overwhelmed teachers to make changes on an individual level, rather than addressing the problem from a broader institutional level. There exists a plentiful supply of data from studies conducted to find the root cause of teacher attrition globally, which lends itself to the calibration of a dynamical system in the hope of offering a nuanced perspective on the problem; possibly offering valuable insight on the key factors contributing to the issue at hand.

The system, discussed in Chapter 2, aims to build on the SIR model proposed by Kermack and McKendrick (1927), combining three systems in order to consider the dynamics at key stages of an individual's teaching career (Early Careers Teacher: ECT, Mid-Stage Teacher: MST, Long-Term Teacher: LTT) to develop a greater understanding of which factors affect one's decision to leave the profession. Analysis will then be undertaken into the steady states of the system, identifying the requirements for stability and classifying the form of each in an effort to spotlight the key parameters which may be exploited to push the population of teachers above government targets in order to maintain a high-quality of mathematics education for secondary school students in England. Following this, we aim to further refine the basic model in Chapter 3 by considering a wider and more developed array of parameters, which allow for class specific parameter values, as well as the development of continuous time-dependent functions which better approximate the recruitment and attrition processes.

Given the significant human influence on the dynamics of our system, we then look to incorporate Reluga, Bauch and Galvani's (2006) work on vaccine uptake based on opinion polling by considering similar game-theoretic techniques in Chapter 4. Following this in Chapter 5, a brief investigation into the generalisability of our investigation will be undertaken to see how the theory and practises discussed throughout this project may be extended to a non-specific workplace; though the education sector has been selected for this project due to the abundance of data available through credible sources such as the government and independent education standard bodies. We then intend to draw conclusions from the analysis undertaken throughout the project to suggest further changes that the Department for Education should undertake to address the crisis based on the analytic form of our steady states and the requirements for stability, briefly considering the feasibility of the implementation of these policies and what further study could take

place to further this inquiry.

2 General Model

As previously discussed, the basis of our model for the teacher population in England is based on the SIR model proposed by Kermach and McKendrick (1927) with the inclusion of time-dependent classes to mimic a two-strain disease (Kuddus *et al.*, 2019) representing individuals who are or are not at risk of leaving the teaching profession. We begin with the formulation of such a system of equations, before moving onto a numerical, and subsequent analytic, investigation regarding the steady states of our system in the hopes of obtaining parameter dependencies which may be exploited to push the number of teachers above government quotas.

2.1 Description and Motivation

In 1927, Kermack and McKendrick proposed a system of equations which would later lay the foundations for the mathematical modelling of infectious diseases, profoundly influencing epidemiology and mathematical biology by establishing the basics of a compartmental framework to describe the dynamics of disease spread through differential equations. Since then, the original system has undergone countless iterations to account for a variety of unique contexts throughout applied mathematics. With regards to the modelling of teacher populations in England, the structure of the SIR model provides a useful starting point, as it captures the dynamic movement of individuals transitioning between different states analogous to the spread of an infectious disease.

In this context, individuals can be categorised as comfortable (analogous to the susceptible group), vulnerable (analogous to the infected group, representing those considering leaving the profession) or removed (representing individuals who have quit or retired). We may then subdivide the comfortable and vulnerable categories into three time-dependent classes, each to account for the notable trends in attrition rates as highlighted in the government census data (Department for Education, 2023b) which illustrates how the largest attrition rates, resulting in a net loss of approximately 40% of the population, occur during the first 10 years of the teaching career. We can represent this by splitting our comfortable and vulnerable categories into three stages in correspondence with the key attrition trends highlighted in the census data:

- C_0, V_0 : Early Career Teachers (Years 0 – 2);
- C_1, V_1 : Mid-Stage Teachers (Years 2 – 10);
- C_2, V_2 : Long-Term Teachers (Years 10+).

This results in a total of 7 populations, as the removed class R remains unchanged.

With our populations clearly defined, we may now outline how individuals move between the 7 classes. Firstly, we note that all individuals enter the system through C_0 , assuming that all ECTs begin with enthusiasm for the career, at some birth rate B . Individuals progress to the subsequent time class, C_{i+1} or V_{i+1} , at a rate α_i after an appropriate amount of time has passed, that time being $\frac{1}{\alpha_i}$ years (i.e. $\alpha_0 = \frac{1}{2}$ and $\alpha_1 = \frac{1}{8}$). Individuals may enter their respective comfortable class from their vulnerable class if they receive sufficient support from their workplace or feel particularly satisfied with their work, this is represented by a support parameter K . Finally, individuals leave the system entirely by entering the removed category R at a rate β , after which they do not return. The details of this model are summarised in Figure 1, which shows a transfer diagram for the basic model, and a discussion of the constraints and physical meanings of each parameter can be found in Section 2.2.

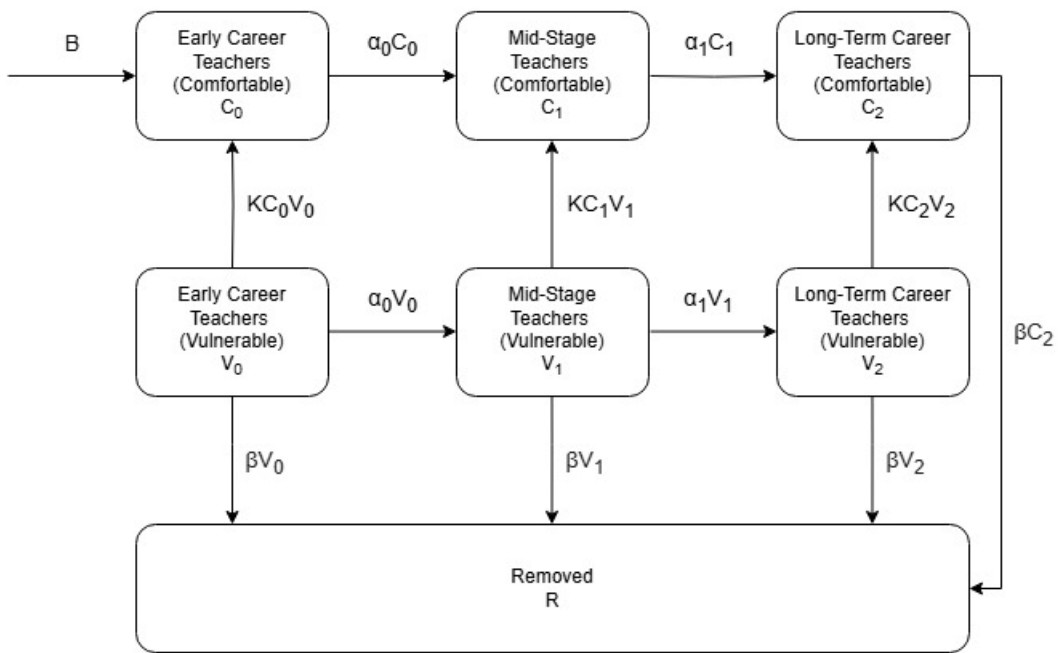


Figure 1: The transfer diagram for the basic model, showing how an individual moves through the system. Notably, all individuals begin in C_0 , move horizontally with respect to time and vertically with respect to the support parameter K , eventually entering R .

From this transfer diagram, we can begin to formulate a system of equations by considering the type of interaction that occurs along each arrow. We begin by asserting that the birth rate is independent of all populations and so, for simplicity, may be represented by some constant $B \in \mathbb{R}^+$. Next we define the horizontal movement throughout the system by $\alpha_i X_i$ where $\alpha_i \in \mathbb{R}^+$ is the rate at which individuals move between job titles (ECT to MST for $i = 0$ and MST to LTT for $i = 1$) and X_i a general population within the system ($X = C$ for the comfortable class and $X = V$ for the vulnerable class), noting that this progression occurs only towards the right. Movement between the comfortable and vulnerable classes is modelled using a Law of Mass Action term $KC_i V_i$ as the two populations mingle throughout the school with some measure of “infectivity” $K \in \mathbb{R}$ which represents the overall support received by teachers at work. It is important to

note that we have chosen to allow $K < 0$ so that the direction in Figure 1 is reversed towards the vulnerable classes if there is insufficient support available. Finally, βX_i for $\beta \in \mathbb{R}^+$ mimics the mortality rate of a disease in the traditional SIR model by being the rate of attrition throughout the system, noting that individuals may only move to the removed category by choosing to quit through the vulnerable classes, or by retiring from C_2 . Using these terms, and the direction of each arrow in our system to decide their signs, we may formulate the following system of equations which will allow us to begin our investigations:

$$\frac{dC_0}{dt} = B - \alpha_0 C_0 + KC_0 V_0 \quad \frac{dV_0}{dt} = -\alpha_0 V_0 - KC_0 V_0 - \beta V_0 \quad (1a)$$

$$\frac{dC_1}{dt} = \alpha_0 C_0 - \alpha_1 C_1 + KC_1 V_1 \quad \frac{dV_1}{dt} = \alpha_0 V_0 - \alpha_1 V_1 - KC_1 V_1 - \beta V_1 \quad (1b)$$

$$\frac{dC_2}{dt} = \alpha_1 C_1 - \beta C_2 + KC_2 V_2 \quad \frac{dV_2}{dt} = \alpha_1 V_1 - KC_2 V_2 - \beta V_2 \quad (1c)$$

$$\frac{dR}{dt} = \beta(V_0 + V_1 + V_2 + C_2) \quad (1d)$$

2.2 Non-Dimensionalisation

To better investigate the model proposed in Section 2.1, we look to rescale the populations into the range $[0, 1]$ so that the values represent percentages of the whole population rather than fixed quantities. The non-dimensionalisation process is near identical for each equation, so we rigorously outline the process for the first pair of equations and simply write the remaining non-dimensionalised equations for brevity. We begin by defining:

$$\tilde{X}_i = \frac{X_i}{N} \quad \text{and} \quad \tau = \frac{t}{T}$$

where:

- X_i is some population from the set $\{C_0, C_1, C_2, V_0, V_1, V_2, R\}$.
- \tilde{X}_i is the new, rescaled, population.
- $N = C_0 + C_1 + C_2 + V_0 + V_1 + V_2 + R$ is the total population of the system.
- τ is the rescaled time variable, however since t is in years already, we simply set $T = 1$ which avoids having to rescale as $\tau = t$.

We then see, via the chain rule^I, that:

$$\frac{d\tilde{X}_i}{dt} = \frac{d\tilde{X}_i}{dX_i} \frac{dX_i}{dt} = \frac{1}{N} \frac{dX_i}{dt}$$

^INote that we do not rescale time as we assume that time is already in years which aligns with our tuning data.

Taking the first pair of Equations (1a), we may substitute the above, to obtain:

$$\begin{aligned}\frac{d\tilde{C}_0}{dt} &= \frac{1}{N}(B - \alpha_0 N \tilde{C}_0 + K N^2 \tilde{C}_0 \tilde{V}_0) = \frac{B}{N} - \alpha_0 \tilde{C}_0 + K N \tilde{C}_0 \tilde{V}_0 \\ \frac{d\tilde{V}_0}{dt} &= \frac{1}{N}(-\alpha_0 N \tilde{V}_0 - K N^2 \tilde{C}_0 \tilde{V}_0 - \alpha_0 N \tilde{V}_0) = -\alpha_0 \tilde{V}_0 - K N \tilde{C}_0 \tilde{V}_0 - \beta_0 \tilde{V}_0.\end{aligned}$$

Carrying out similar manipulations on the remaining 5 equations from (1), we notice that the only meaningful change occurs with the birthrate B which becomes $\frac{B}{N}$ and K which becomes KN . For clarity, the tilde will be dropped in the non-dimensionalised terms, thus after rescaling our entire system, we are left with our new set of equations:

$$\frac{dC_0}{dt} = \frac{B}{N} - \alpha_0 C_0 + K N C_0 V_0 \quad \frac{dV_0}{dt} = -\alpha_0 V_0 - K N C_0 V_0 - \beta V_0 \quad (2a)$$

$$\frac{dC_1}{dt} = \alpha_0 C_0 - \alpha_1 C_1 + K N C_1 V_1 \quad \frac{dV_1}{dt} = \alpha_0 V_0 - \alpha_1 V_1 - K N C_1 V_1 - \beta V_1 \quad (2b)$$

$$\frac{dC_2}{dt} = \alpha_1 C_1 - \beta C_2 + K N C_2 V_2 \quad \frac{dV_2}{dt} = \alpha_1 V_1 - K N C_2 V_2 - \beta V_2 \quad (2c)$$

$$\frac{dR}{dt} = \beta(V_0 + V_1 + V_2 + C_2) \quad (2d)$$

where:

- B is the birthrate for the system, representing the number of newly employed teachers each year.
- $\alpha_i \in [0, 1]$ are the rates at which individuals transition between classes with respect to time; by construction we have $\alpha_0 = \frac{1}{2}, \alpha_1 = \frac{1}{8}$.
- $\beta \in [0, 1]$ is the attrition rate, representing the rate at which individuals quit/retire from the profession.
- $K \in [-1, 1]$ is the support parameter, which represents the rate at which individuals move between classes vertically (towards V_i when $K < 0$ or towards C_i when $K > 0$). This term represents the support an individual receives from their workplace as well as accounting for psychological factors such as job satisfaction, financial incentives, emotional well-being, etc.

An exploration of these parameters, with greater detail on the factors influencing their value, can be found in Chapter 3 where we consider more refined forms of these parameters including class-specific support parameters and time-dependent functions to further develop our model.

Note that, by summing the non-dimensionalised system in Equations 2, we find the

change in the total teaching population to be

$$\frac{dN}{dt} = \frac{B}{N}$$

thus, the total teacher population is only constant when there is no input to the system (i.e. $B = 0$). However, given the structure of our system, this would mean that in finite time, all individuals eventually enter the removed class – leaving no working individuals in our model. To account for this, we may instead consider N_w as the working population, ignoring the removed class such that:

$$N_w = C_0 + C_1 + C_2 + V_0 + V_1 + V_2$$

with

$$\frac{dN_w}{dt} = \frac{B}{N} - \beta(V_0 + V_1 + V_2 + C_2)$$

thus, for a constant working population N_w , we require:

$$\frac{B}{N} = \beta(V_0 + V_1 + V_2 + C_2)$$

Limitations of The Basic Model:

Before continuing with our analysis, it is worth considering the limitations of the model and where it might fail to accurately represent the real-life scenario:

1. The attrition rate β clearly varies with respect to time, as highlighted in the work-force census (Department for Education, 2023b), to account for this, we later consider class specific and time dependent attrition rates tuned by the census data in Section 3.1.
2. The system's input B will, in reality, fluctuate throughout the year, peaking in September as the school year begins when most individuals enter the system. For now it is a sufficient approximation, but a periodic function is proposed in Section 3.2.
3. The support parameter K may in fact vary between the 3 career stages (ECTs may receive extra support from experienced members of faculty whilst veteran teachers receive less support in comparison) and is affected by a multitude of social, economic and psychological factors that are beyond the scope of this project entirely. However, a brief investigation is undertaken in Section 3.3.

Despite these pitfalls, the basic model proposed in Equations (2) provides a suitable starting point for our investigations, encapsulating the key dynamics of our system and allowing preliminary analysis to be undertaken into the long-term behaviours of our system, which we may later refine after determining the validity of our system.

2.3 Numerical Investigations

To verify the validity of our basic model outlined in Section 2.2, using Python to plot the solutions $X_i(t)$, we look to conduct a series of numerical investigations where we aim to observe the solution trajectories expressing behaviours that we would expect to see from our research and intuition. Using SciPy's `solve_ivp` function (see Appendix B for the full code), we are able to plot the populations $X_i(t)$ for various parameter configurations. In order to better investigate the effects of varying each parameter, specifically $K \in [-1, 1]$. All instances of the code are initialised with the following parameter, and initial, values for consistency:

- $\beta = 0.2$: chosen arbitrarily prior to tuning.
- $\frac{B}{N} = \beta(V_0 + V_1 + V_2 + C_2)$: this allows for a constant working population, mimicking a closed system when R is excluded.
- $X_i(0) = \frac{1}{6}$ for all $X_i(t) \in \{C_0(t), C_1(t), C_2(t), V_0(t), V_1(t), V_2(t)\}$: for simplicity, we assume that the population is uniformly distributed among the working populations.
- $R(0) = 0$: as the working populations have no R dependency and all populations eventually lead to R , we have the class start empty, as it has no effect on the remaining system.

Model Validation for a Closed System ($B = 0$):

To verify that movement through our transfer diagram is appropriately expressed in our model system, we begin by setting the input of our system to zero to observe the case where no new individuals enter the population. Figure 2 shows the behaviour we expect to see, as all working populations tend to zero in finite time as all movement leads towards the removed class, which tends to one, verifying the proposed dynamics and parameter choices of our model.

We note that, since all individuals eventually enter and remain in the removed class R , we always see the removed population tend to one in finite time. For that reason, the plot for R will be withheld in future plots to avoid cluttering figures with irrelevant information.

Varying Support for a Fixed Working Population ($B \neq 0$, $K \in [-1, 1]$):

We now look at the case for $B \neq 0$, specifically B such that the working population remains fixed, by setting:

$$\frac{B}{N} = \beta(V_0 + V_1 + V_2 + C_2)$$

and consider how the behaviour of our numerical solutions change as K is varied continuously through the interval $[-1, 1]$. By fixing the working population, we are able to

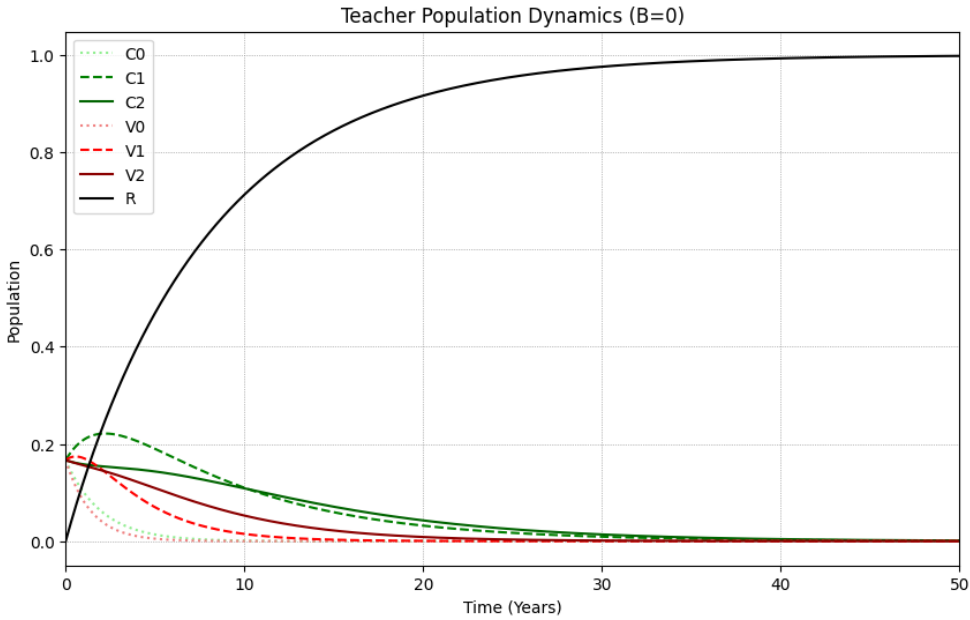


Figure 2: Plot of the basic model's solution trajectories showing that with $B = 0$ and $K = 0$, all working populations tend to 0 whilst the removed class tends to 1 in finite time. Analogous behaviours occur for any $K \in [-1, 1]$.

investigate how the steady states of our system depend on K without the influence of varying the size of the working population. In particular, the overarching goal of our investigation is to find K such that $C_2 \gg V_2$, in order to ensure a quality education is delivered to students and avoid any harmful effects to the wider teacher population, and to further justify our physical interpretation of the parameter being a measure of support, in order to better inform the proposed policy changes in Section 6.3.

$$K \in (0, 1]$$

We begin by considering the optimal case where $K \in (0, 1]$, representing the situation in which teachers receive a plentiful support and are overall satisfied with their career. A numerical approximation of this situation can be seen in Figure 3 which shows all three comfortable solution trajectories converging in finite time to a fixed limit value, indicating the presence of three corresponding stable steady states. Similarly, all three vulnerable states rapidly decay to zero suggesting that all vulnerable populations tend to 0. This rapid decay to zero is entirely expected, further validating the model structure, as there is no input into the vulnerable classes directly. Individuals only become vulnerable after receiving insufficient support, and hence we would expect the respective populations to decay to zero due to the structure of our model which pushes all individuals towards the removed class in finite time. Curiously, the intermediate C_1 class remains the largest of the non-zero populations, further investigations in Section 2.4 will justify this, but for now we intuitively assume this is because C_2 has a retiring rate which subtracts from the total population whilst C_1 only loses population at a much lower rate as individuals transition forward in time.

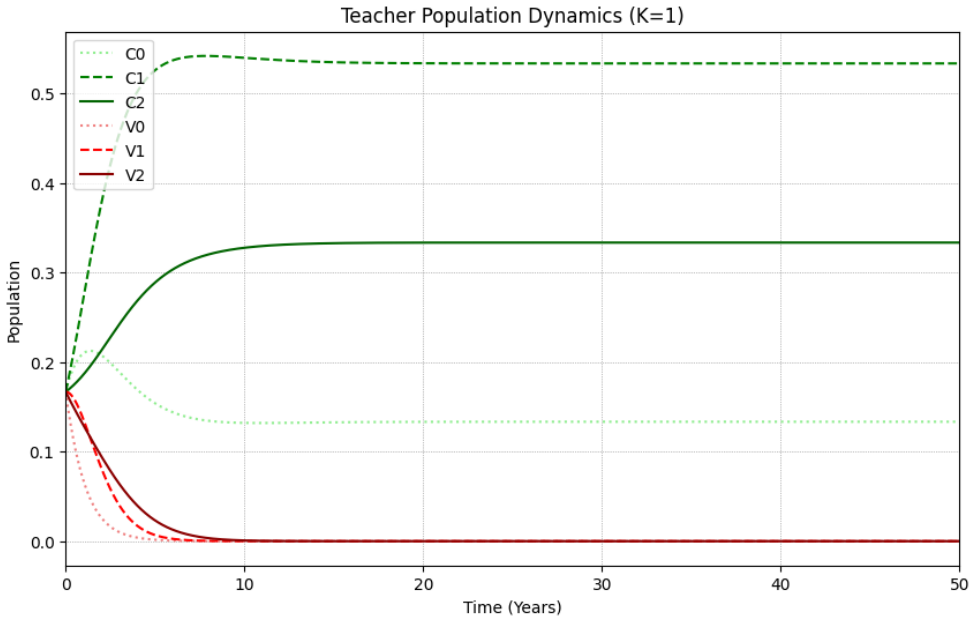


Figure 3: Plot of the basic model's solution trajectories for $K = 1$, showing that the comfortable steady states, C_0, C_1, C_2 dominate.

$K = 0$

Decreasing K so that it eventually reaches zero yields Figure 4, this being the case where teachers are indifferent to their career, and so no movement occurs between the comfortable and vulnerable classes. The lack of vertical movement in the model results in the separation of the system in which the comfortable states tend to some steady state values and the vulnerable states decay to zero once again. This is to be expected as we had previously assumed new teachers only enter the system via C_0 and so the vulnerable system has no input and behaves similarly to the $K \in (0, 1]$ case, with all individuals eventually entering R , albeit slower this time as there is no additional removal term.

$K \in [-1, 0)$

Finally, we look at the case where $K \in [-1, 0)$, shown in Figure 5, representing when teachers are receiving insufficient support or feel particularly dissatisfied with their career. As we decrease K through the negative portion of the interval, we see that the comfortable and vulnerable states begin to gradually swap places, crossing some critical K^* (around -0.25 for this particular case) where $V_2 > C_2$ for all $K \in [-1, K^*]$. Contrary to the dynamics explored in the positive interval, which appeared to monotonically approach their steady state values, we now see non-monotonic approaches that require analytic investigations to comment on the long-time behaviours of the system. More broadly however, we may comment on the existence of some K^* which will play a key role as a threshold value for which $K \in (K^*, 1]$ forces the model to favour comfortable teacher populations at steady state.

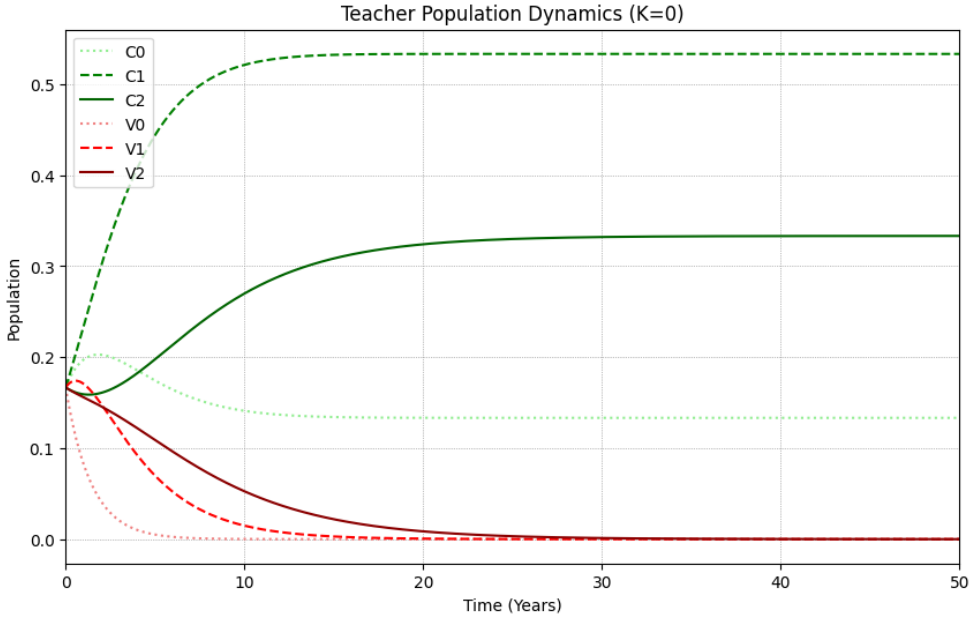


Figure 4: Plot of the basic model’s solution trajectories for $K = 0$, showing a similar picture to Figure 3 but stretched slightly in the time direction.

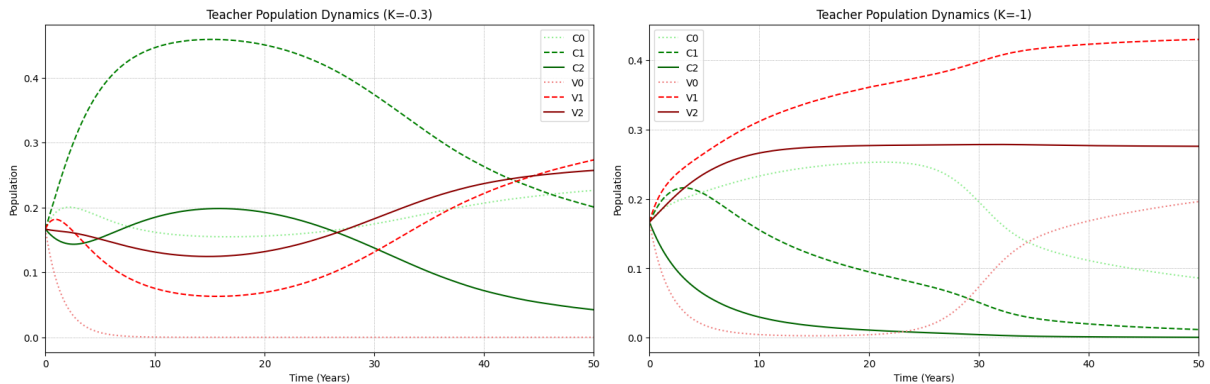


Figure 5: Plots of the basic model’s solution trajectories for $K = -0.3$ (left) and $K = -1$ (right) which shows the comfortable states decreasing and the vulnerable states increasing as $K \rightarrow -1$.

2.4 Steady State Analysis

With our model verified numerically, we now look to investigate the analytic form of the steady states for the system, these being the points \mathbf{X}_i^* such that $\frac{d\mathbf{X}_i}{dt}|_{\mathbf{X}_i^*} = 0$ where $\mathbf{X}_i^* = (C_0^*, C_1^*, C_2^*, V_0^*, V_1^*, V_2^*)$ is the vector of steady state values (note that all the values in the vector \mathbf{X}_i^* are between 0 and 1). In order to identify these, we used Maple to simplify the lengthy algebraic procedures. This led to the identification of four possible cases:

$$\text{Case 1: } \left(\frac{B}{N\alpha_0}, \frac{B}{N\alpha_1}, \frac{B}{N\beta}, 0, 0, 0 \right)$$

$$\text{Case 2: } \left(\frac{B}{N\alpha_0}, \frac{B}{N\alpha_1}, -\frac{\beta}{KN}, 0, 0, \frac{BK + \beta^2}{KN\beta} \right)$$

$$\text{Case 3 \& 4: } \left(\frac{B}{N\alpha_0}, -\frac{\alpha_1 + \beta}{KN}, \frac{X \pm \sqrt{Z}}{Y}, 0, \frac{BK + \alpha_1^2 + \beta\alpha_1}{\frac{1}{2\beta}Y}, \frac{\beta [2\alpha_1(\alpha_1 + \beta)^2 + X \pm \sqrt{Z}]}{NK(X \pm \sqrt{Z})} \right)$$

where $X = BK\alpha_1 - \alpha_1^2\beta - 2\alpha_1\beta^2 - \beta^3$ and $Y = 2NK\beta(\alpha_1 + \beta)$ and $Z = X^2 - 4\alpha_1\beta^2(\alpha_1 + \beta)^3$.

Note that Case 3 is the positive case and Case 4 the negative case of the final expression. To ensure that our solution vector \mathbf{X}_i^* is realistic according to the physical constraints of our problem, we must enforce that each element of the steady state vectors be non-negative. To do this, we notice that each parameter in the system of equations (2) is non-negative except for $K \in [-1, 1]$; thus we look to form existence conditions for each of the above cases in terms of the support parameter K .

Case 1: We immediately see that each element is non-negative and has no dependencies on the parameter K , as such we immediately conclude that Case 1 holds for the entire interval

$$K \in [-1, 1] =: I_1$$

Case 2: For all elements of the steady state vector to be non-negative, we define relations on the parameter K , only the third and final elements have dependencies on K and so starting with the third element we require:

$$-\frac{\beta}{KN} \geq 0 \implies K < 0$$

since $\beta, N \geq 0$. We then use the additional condition that $K < 0$, to obtain the following condition on the final element to obtain:

$$\frac{BK + \beta^2}{KN\beta} \geq 0 \implies BK + \beta^2 \leq 0 \implies K \leq -\frac{\beta^2}{B} < 0.$$

Thus, for Case 2 to exist, we require that K satisfy both inequalities, forming the final interval:

$$K \in \left[-1, -\frac{\beta^2}{B} \right] =: I_2$$

Cases 3 & 4: Just as before, we notice that all but two elements depend on K , defining conditions for each element sequentially, we firstly require the second element to be non-negative:

$$-\frac{\alpha_1 + \beta}{KN} \geq 0 \implies K < 0$$

since $\alpha_1, \beta \geq 0$. Next we require the third element to be non-negative such that:

$$\frac{X \pm \sqrt{Z}}{Y} \geq 0.$$

We see that within the expressions for $Z = X^2 - 4\beta^2\alpha_1(\alpha_1 + \beta)^3$, we have:

$$\mathcal{O}(10^{-3}) = X^2 \gg 4\beta^2\alpha_1(\alpha_1 + \beta)^3 = \mathcal{O}(10^{-6})$$

and so, to simplify our analysis by focusing on the overall behaviours of our model, we may ignore the small terms and approximate $Z \approx X^2$ throughout this project, hence $\sqrt{Z} \approx \sqrt{X^2} = |X|$. To prove non-negativity of this expression, we see $Y = 2NK\beta(\alpha_1 + \beta) < 0$ (since $K < 0$), and obtain the following expression:

$$\frac{X \pm |X|}{Y} \geq 0 \implies X \pm |X| \leq 0.$$

This can only be true for the subtraction case when $X < 0$, while it is only true in the addition case when $X = 0$, which cannot hold in order to avoid a division by 0 in the last element of the steady state vector, thus Case 3 cannot be considered biologically realistic and will be removed from all future analysis.

Returning to the original expression, but only for Case 4 (the minus case), we can then find a condition on K such that $X < 0$:

$$X = BK\alpha_1 - \alpha_1^2\beta - 2\alpha_1\beta^2 - \beta^3 < 0 \implies K < \frac{\alpha_1^2\beta + 2\alpha_1\beta^2 + \beta^3}{B\alpha_1}.$$

Considering the next element of the steady state vector with the additional condition $K < 0$, we then require:

$$\frac{BK + \alpha_1^2 + \beta\alpha_1}{KN(\alpha_1 + \beta)} \geq 0 \implies BK + \alpha_1^2 + \beta\alpha_1 \leq 0 \implies K \leq -\frac{\alpha_1(\alpha_1 + \beta)}{B}$$

and investigating the final element of the vector, we require:

$$\frac{\beta [2\alpha_1(\alpha_1 + \beta)^2 + X - \sqrt{Z}]}{NK(X - \sqrt{Z})} \geq 0$$

which, using the approximation $Z \approx X^2$ simplifies to:

$$\frac{\beta [2\alpha_1(\alpha_1 + \beta)^2 + X - |X|]}{NK(X - |X|)} \geq 0.$$

Since $K < 0$, it follows that $X < 0$, allowing us to set $|X| = -X$ by definition, and thus to satisfy the above inequality it suffices to show the numerator is positive:

$$\begin{aligned} 2\alpha_1(\alpha_1 + \beta)^2 + X - |X| &= 2\alpha_1(\alpha_1 + \beta)^2 + 2X \geq 0 \\ \implies \alpha_1(\alpha_1 + \beta)^2 &\geq -X \end{aligned}$$

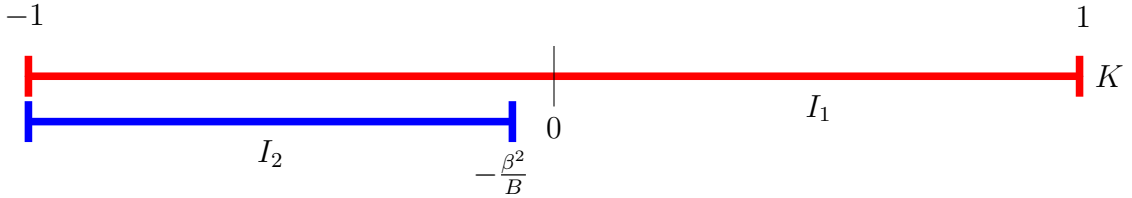


Figure 6: A number line showing the two intervals of existence for Cases 1&2 identified in Section 2.4.

Returning to the original expression for X we can then form the final condition on K :

$$\begin{aligned} \alpha_1(\alpha_1 + \beta)^2 &\geq -BK\alpha_1 + \alpha_1^2\beta + 2\alpha_1\beta^2 + \beta^3 = -X \\ \implies \frac{\beta^3 + \alpha_1\beta^2 - \alpha_1^2\beta - \alpha_1^3}{B\alpha_1} &\leq K \end{aligned}$$

where the numerator of the left-hand expression simplifies to $(\beta - \alpha_1)(\alpha_1 + \beta)^2$. Therefore, this gives two conditions on K ,

$$\frac{(\beta - \alpha_1)(\alpha_1 + \beta)^2}{B\alpha_1} \leq K \quad \text{and} \quad K \leq -\frac{\alpha_1(\alpha_1 + \beta)}{B}.$$

To identify the interval which covers this entire case, we look at the intersection of these inequalities, to do this we must ensure that the upper and lower bounds of K are indeed that, this means checking:

$$\begin{aligned} \frac{(\beta - \alpha_1)(\alpha_1 + \beta)^2}{B\alpha_1} &\leq -\frac{\alpha_1(\alpha_1 + \beta)}{B} \\ \implies \beta^2 - \alpha_1^2 &= (\beta - \alpha_1)(\alpha_1 + \beta) \leq -\alpha_1^2 \\ \implies \beta^2 &\leq 0 \end{aligned}$$

which cannot hold as $\beta > 0$ by construction. Thus we conclude that there cannot exist an interval for this case to exist and thus Case 4 will also be removed from all future analysis due to its biological infeasibility.

Extra Case 5: A fifth, incredibly lengthy, steady state was also identified, though it has been withheld from this project as it is unfeasible to investigate analytically. However, through our investigations, we posit that it may theoretically exist for $K \approx -1$.

The different cases and their intervals of existence are summarised in Figure 6.

2.5 Stability Analysis

To identify the stability of the steady states outlined in Section 2.4, we look to analyse the signs of the eigenvalues generated by the 6×6 Jacobian matrix, J :

$$J = \begin{bmatrix} KNV_0 - \alpha_0 & KNC_0 & 0 & 0 & 0 & 0 \\ -KNV_0 & -KNC_0 - \alpha_0 - \beta & 0 & 0 & 0 & 0 \\ \alpha_0 & 0 & KNV_1 - \alpha_1 & KNC_1 & 0 & 0 \\ 0 & \alpha_0 & -KNV_1 & -KNC_1 - \alpha_1 - \beta & 0 & 0 \\ 0 & 0 & \alpha_1 & 0 & KNV_2 - \beta & KNC_2 \\ 0 & 0 & 0 & \alpha_1 & -KNV_2 & -KNC_2 - \beta \end{bmatrix}$$

With the ordering $[C_0, V_0, C_1, V_1, C_2, V_2]$ for clarity of matrix representation, opposed to the previous ordering $[C_0, C_1, C_2, V_0, V_1, V_2]$.

Finding the eigenvalues of the matrix J by solving $\det(J - \lambda I) = 0$ where I is the identity matrix, we obtain the following list of six eigenvalues in terms of C_i, V_i for our system before considering their values in the previously discussed cases:

$$\begin{aligned} \lambda_1 &= -\beta \\ \lambda_2 &= -KN(C_2 - V_2) - \beta \\ \lambda_3 &= \frac{KNX_0^- - \beta - 2\alpha_0 + \sqrt{P_0(K)}}{2} \\ \lambda_4 &= \frac{KNX_0^- - \beta - 2\alpha_0 - \sqrt{P_0(K)}}{2} \\ \lambda_5 &= \frac{KNX_1^- - \beta - 2\alpha_1 + \sqrt{P_1(K)}}{2} \\ \lambda_6 &= \frac{KNX_1^- - \beta - 2\alpha_1 - \sqrt{P_1(K)}}{2} \end{aligned}$$

where:

$$X_i^+ = V_i + C_i, \quad X_i^- = V_i - C_i \quad P_i(K) := (KNX_i^-)^2 + 2KN\beta X_i^+ + \beta^2 \quad \text{for } i = 0, 1.$$

For an eigenvalue to correspond to a stable direction, we require $\Re(\lambda) < 0$. We observe that this is always satisfied for the first eigenvalue $\lambda_1 = -\beta$ as $\beta > 0$. However, determining the stability of the remaining five eigenvalues requires further analysis, particularly in relation to the ratio of steady state values C_i^* to V_i^* and the support parameter K . Since the first eigenvalue is always stable, we may immediately conclude all steady states are either locally asymptotically stable or a saddle node with at least one stable direction. Whilst a detailed classification of each steady state (e.g., node, focus or centre) is unnecessary for the purposes of this project, a brief investigation into the conditions under which each eigenvalue has negative real parts provides a robust justification for the local behaviour of the model by analysing the linearised system.

To analyse the sign of each λ , we will consider three distinct cases, those being when our support parameter K is positive, negative or zero. This will then allow us to classify

the possible number of stable eigenvalues in each of the four cases previously defined in Section 2.4.

$\lambda_2 = -\mathbf{K}\mathbf{N}(\mathbf{C}_2 - \mathbf{V}_2) - \boldsymbol{\beta}$: For $\lambda_2 < 0$, as this eigenvalue is always real by construction, we simply require:

$$\begin{cases} V_2 - C_2 < \frac{\beta}{KN}, & K > 0 \\ V_2 - C_2 > \frac{\beta}{KN}, & K < 0 \end{cases}$$

for stability. We also note that in the case where $K = 0$, the eigenvalue reduces to $\lambda_2 = -\beta$ which is always stable by construction. In the $K > 0$ case, the difference can be negative, suggesting that we require either C_2 much larger than V_2 at steady state, or that their difference is sufficiently small and positive. In the other case $K < 0$, their difference is bounded below by a negative quantity, suggesting that there is a small range for C_2 to be larger than V_2 at steady state, but otherwise their difference may be positive and still obtain stability.

$\lambda_{3,4,5,6} = \frac{KNX_i^- - \beta - 2\alpha_1 \pm \sqrt{P_i(K)}}{2}$ for $i = 0, 1$: For the remaining four cases, we see that they split into two equivalent situations where we consider the \pm cases for $i = 0, 1$, as such we will only consider the $i = 1$ cases as the others are identical up to a different index. Since we are investigating the situation in which $\Re(\lambda_i) < 0$, we notice that when the interior of the square root is negative, i.e

$$P_1(K) := (KNX_1^-)^2 + 2KN\beta X_1^+ + \beta^2 \leq 0.$$

Using the quadratic formula, the function $P_1(K)$ has roots at:

$$K_{\pm}^{(1)} = \frac{\beta}{(X_1^-)^2} \left(X_1^+ \pm \sqrt{(X_1^+)^2 - (X_1^-)^2} \right).$$

The only real part of our eigenvalue is what lies outside of the square root, as the interior becomes purely imaginary, and hence we are left with finding when:

$$KNX_1^- - \beta - 2\alpha_1 < 0$$

with the additional constraint that $K \in [K_-, K_+]$ so that $P_1(K) \leq 0$ is satisfied. Again, considering the situation depending on the sign of K we obtain that these eigenvalues have negative real part when either of the following hold:

$$\begin{cases} V_1 - C_1 < \frac{\beta+2\alpha_1}{KN}, & K \in (0, 1] \cap [K_-^{(1)}, K_+^{(1)}] \\ V_1 - C_1 > \frac{\beta+2\alpha_1}{KN}, & K \in [-1, 0) \cap [K_-^{(1)}, K_+^{(1)}] \end{cases}$$

Now looking at the other case when $P_1(K) \geq 0$ so that the whole expression is real, we require:

$$\begin{aligned} & \pm \sqrt{P_1(K)} + KNX_1^- - \beta - 2\alpha_1 < 0 \\ \implies & Q_1(K) := \pm \sqrt{P_1(K)} + KNX_1^- < \beta + 2\alpha_1 \end{aligned}$$

which has been left in general terms of a polynomial $Q_1(K)$ for simplicity with the addi-

tional constraint that:

$$P_1(K) > 0 \implies K \in [-1, K_-^{(1)}) \cup (K_+^{(1)}, 1]$$

To conclude, we consider the case when $K = 0$, substituting this into the original expression for λ we obtain:

$$\lambda = \frac{\pm\sqrt{\beta^2 - \beta - 2\alpha_1}}{2} = \frac{\pm|\beta| - \beta - 2\alpha_1}{2}$$

$$\lambda_{3,4,5,6} = -\alpha_1, -(\alpha_1 + \beta)$$

which are both strictly negative, hence when $K = 0$, all steady states are locally asymptotically stable.

Summarising this in Table 1, we have the following conditions for each eigenvalue of the Jacobian J to have negative real part.

Eigenvalues	Inequality	Interval
$\lambda_1 < 0$		always true
$\lambda_2 < 0$	$V_2 - C_2 < \frac{B}{KN}$	$K > 0$
	$V_2 - C_2 > \frac{B}{KN}$	$K < 0$
$\lambda_{3,4} < 0$	$V_1 - C_1 < \frac{\beta+2\alpha_1}{KN}$	$K \in (0, 1] \cap [K_-^{(1)}, K_+^{(1)}]$
	$V_1 - C_1 > \frac{\beta+2\alpha_1}{KN}$	$K \in [-1, 0) \cap [K_-^{(1)}, K_+^{(1)}]$
	$Q_1(K) < \beta + 2\alpha_1$	$K \in [-1, K_-^{(1)}) \cup (K_+^{(1)}, 1]$
$\lambda_{5,6} < 0$	$V_0 - C_0 < \frac{\beta+2\alpha_0}{KN}$	$K \in (0, 1] \cap [K_-^{(0)}, K_+^{(0)}]$
	$V_0 - C_0 > \frac{\beta+2\alpha_0}{KN}$	$K \in [-1, 0) \cap [K_-^{(0)}, K_+^{(0)}]$
	$Q_0(K) < \beta + 2\alpha_0$	$K \in [-1, K_-^{(0)}) \cup (K_+^{(0)}, 1]$

Table 1: A list of conditions required for each eigenvalue to be negative.

From this we can conclude that a steady state is asymptotically stable when K satisfies all of the above conditions; otherwise it is a saddle with as many stable directions as there are negative eigenvalues depending on how many of the above conditions are satisfied by K . However, by comparing the intervals of K , we see a partition of the admissible set

$[-1, 1]$ into $[-1, 0]$ and $(0, 1]$ making it impossible for a single steady state to satisfy all of the above criteria for $K \neq 0$. Thus we may conclude that all steady states are saddles for $K \in [-1, 0) \cup (0, 1]$ and locally asymptotically stable when $K = 0$.

2.6 Parameter Investigations

With the steady states of the basic system (2) identified in Section 2.4 and classified in Section 2.5, we can now look to select parameters β and B to maximise the C_2 steady state and minimise the V_0 , V_1 and V_2 steady states so that the working population mostly consists of individuals in the C_2 population. To do this, we will take fixed values of $K \in [-1, 1]$ and N such that the steady state solutions to our problem exist in the two distinct cases identified at the end of Section 2.4, and assume such values of K satisfy the necessary stability conditions as identified at the end of Section 2.5 – allowing us to focus our efforts towards choosing β and B effectively.

Case 1: $\left(\frac{B}{N\alpha_0}, \frac{B}{N\alpha_1}, \frac{B}{N\beta}, 0, 0, 0 \right)$

For the first case, we note that to maximise

$$C_2 = \frac{B}{N\beta},$$

we simply maximise B and minimise β . Contextually, this means that when K is positive or small and negative, an effort should be made to increase recruitment and retention, as the system in its current state is a healthy enough work environment to support new individuals without risking the well-being of the wider population.

Case 2: $\left(\frac{B}{N\alpha_0}, \frac{B}{N\alpha_1}, -\frac{\beta}{KN}, 0, 0, \frac{BK+\beta^2}{KN\beta} \right)$

Taking note of the fact that $K < 0$ in this case, we first look to maximise

$$C_2 = -\frac{\beta}{KN},$$

which simply results in maximising β , in contrast to the previous case, this equates to worsening attrition rates. Perhaps in an attempt to better devote the limited resources available, the system must let the total population reduce to a more manageable size by allowing individuals leave the system.

Looking next to minimise

$$V_2 = \frac{BK + \beta^2}{KN\beta},$$

we let $\beta = 1$ to simulate the optimised C_2 as above, giving

$$V_2 = \frac{BK + 1}{KN} = \frac{B}{N} + \frac{1}{KN}$$

which may be minimised by taking B small. This once again opposes the conclusions of

Case 1 by discouraging recruitment efforts, though this agrees with the earlier intuition that the population is somehow oversaturated and must be reduced due to the lack of support resources available in an attempt to create a healthier working environment.

In summary, we see that Case 1 may be optimised by choosing B large, which may be done by promoting recruitment campaigns by groups such as *Teach First* or *Get into Teaching* and making the career more attractive to potential applicants, for example, by increasing salary so that individuals are more drawn to the career; and by choosing β small, so that more individuals remain in the career for longer, making use of the abundance of support resources available to them as K is typically positive in this case. Similarly, we see that Case 2, where $K < 0$, can be optimised by choosing B small and β large in direct contrast to Case 1. Intuitively, we may assume that when $K < 0$, recruitment campaigns should be reduced as the workforce is already struggling, and so increasing the total population size would further reduce the amount of support available to each individual. Similarly a high attrition rate is required to lower the total workforce's size so that the limited resources may be better distributed amongst the remaining teachers. Being able to manage these changes does however require the Department for Education to have a greater awareness of the system as a whole, monitoring K through regular surveys and adjusting their retention strategies accordingly to ensure they meet their targets.

Ultimately from our analysis, we see that the ideal case is of course when $K > -\frac{\beta^2}{B}$ such that we are in Case 1 where all vulnerable steady states tend to 0. However, we have identified the condition for which the remaining case may be optimised to ensure the best case scenario in the event of insufficient support. Specific ideas for new policies that enforce these optimal conditions are briefly discussed in Section 2.6 where the analysis undertaken here is used as justification for our suggestions.

3 Extended Model

With the basic model from Equations (2) sufficiently investigated for the purposes of optimising the steady states of our system, we now return to the ideas presented in Section 2.2 and extend the initial system of equations by considering functional replacements of our original parameters. This chapter aims to explore a series of theoretical extensions to the basic model proposed in Chapter 2. While the original model assumes the parameters B, β and K to be fixed, we now consider time-dependent and functional forms which may better capture the dynamics of complex professional environments.

Specifically, we will introduce a time-dependent attrition rate, tuned by government census data (Department for Education, 2023b) to create a polynomial interpolant which best approximates teacher attrition trends. Similarly, we will use government hiring data to inform the creation of a sinusoidal birthrate function that accounts for the increase in hiring targets each year. Additionally, we will propose a functional support term which considers the many psychological and financial influences that affect an individual's decision to remain in the profession.

This chapter greatly focuses on exploration over formal implementation, stability anal-

ysis or simulation of the presented extensions. This brief discussion aims to establish a conceptual understanding for future work which could include such extensions in their dynamics.

3.1 Time-Dependent β_i

The basic model proposed in Chapter 2 assumes the attrition rate of our system β to be constant and fixed for each population irrespective of the duration an individual has been teaching, inaccurately suggesting that teachers of 1 and 50 years experience have the same chance of leaving at a given time t . Whilst this simplifies the analysis of our model and provides a good starting point for our system of equations, this is an obvious oversimplification which may be easily expanded upon to further develop the model system. In this section, we will briefly propose two alternatives to this based on real-world data that will increase the accuracy of our model.

To better model the attrition rate β within our system (Equations (2)), we can look to account for the variations in this parameter value that may occur as time progresses. Using data from the 2023 workforce census (Department for Education, 2023b), we may begin to tune β to better fit the context of our model. Firstly, one could define β_0, β_1 and β_2 as the respective attrition rates for each population, V_0, V_1 and V_2 , respectively; as well as a β_r in C_2 which accounts for those individuals who reach the age of retirement and leave the workforce naturally rather than through dissatisfaction. Using census data for 2023, we can obtain the values for β_0, β_1 and β_2 by averaging the percentage of individuals who leave in each time frame. This gives:

$$\beta_0 = 0.154, \quad \beta_1 = 0.316, \quad \beta_2 = 0.505.$$

To obtain β_r , we can then use pension scheme data from the same census to obtain the number of full-time teachers that retired in 2022/2023 and divide that by the total number of full-time teachers in the workforce that year to obtain the percentage of individuals who retired:

$$\beta_r = \frac{\text{Number of Retirees}}{\text{Total Number of Teachers}} = \frac{4793}{468693} = 0.010.$$

Note that the teacher pension scheme data from 2023 shows that all but 3 individuals retired after the age of 40, allowing us to comfortably assume, for the purposes of our model, that we need only include a retiring term in the C_2 equation.

Although tuning the parameters of our system to averaged data helps to somewhat better fit our solutions, we may extend our approximations beyond this and replace β altogether with a time-dependent function $\beta(t)$ which uses the entire data set to produce a polynomial interpolant. To do this, we use Python's SciPy `curve_fit` function which takes in the workforce census data and, using a least squares optimisation method, returns a polynomial $P_N(t)$ of degree N which approximates the provided data points. To avoid numerical instabilities, we choose N to be relatively small (e.g. $N < 5$). Testing this for $N = 2, 3, 4$ we obtain the graphs in Figure 7.

From Figure 7 we see, as expected, that the polynomial interpolants with even powers

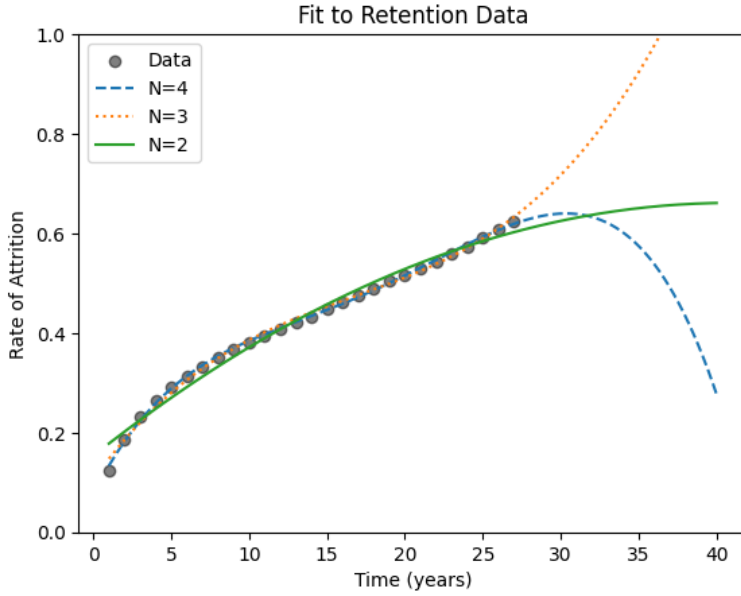


Figure 7: Plots of polynomial interpolates for retention data of degree 3,4 and 5.

have global maxima within the career time frame identified from the government census data of roughly 40 years (Department for Education, 2023b) meaning that there exist points $t_2^*, t_4^* > 0$ such that $P_2(t_2^*) = P_4(t_4^*) = 0$ where the subscript denotes the degree of the polynomial interpolant. In contrast to this, we note that the cubic case is well behaved, interpolating the data with moderate accuracy while also reaching $\beta = 1$ in finite time, representing the realistic limit of our attrition function, since individuals cannot remain in the system forever. Using this, we can then define our final attrition function as, for any fixed $t > 0$:

$$\beta(t) = \min\{P_3(t), 1\}$$

$$\text{where } P_3(t) = (3.91 \cdot 10^{-5})t^3 - (1.95 \cdot 10^{-3})t^2 + (4.36 \cdot 10^{-2})t^2 + 0.11.$$

Implementing this into the basic model proposed in Chapter 2, we can simply replace our parameter β by the discrete time approximation $\beta(t)$, and take limits of our equations under the assumption that steady states exist such that for any population X^{II} in our, system we have:

$$\lim_{t \rightarrow \infty} \frac{dX}{dt} = 0.$$

Given the structure of our function $\beta(t)$ we see that:

$$\lim_{t \rightarrow \infty} \beta(t) = 1$$

Thus it suffices to replace any instance of β in our analysis by 1 instead, essentially eliminating the attrition rate. In doing this, one may interpret the parameter β not as the percentage of individuals leaving in a given year, but now as the probability of a single individual leaving in a given year. This shift from population-wide to individual-

^{II}Where $X \in \{C_0, C_1, C_2, V_0, V_1, V_2\}$.

specific is a necessary observation to make, as otherwise it may be mistakenly assumed that (according to Figure 7) after around 35 years 100% of the teaching population are leaving each year.

3.2 Functional Birth Rate $B(t)$

Taking a more micro-scale approach compared to the macro-scale of Section 3.1, we look to replace the constant birthrate term B with a periodic function that oscillates throughout the year to mimic the hiring patterns of teachers with respect to the academic year. To do this, we consider a sinusoidal function whose local maxima coincide with the start of the academic calendar, September. To begin with, we consider the function:

$$B_1(t) := \sin\left(2\pi\left(t + \frac{1}{2}\right)\right) + 1$$

shown in Figure 8, this simply translates the curve in the t -axis to account for the desired maxima locations, and translates the curve up to ensure non-negativity.

Building on this, we may account for teacher retraining, a popular method used in schools to help mitigate the lack of mathematics teachers available which involves having other subject teachers reskill and specialise into mathematics as a secondary subject. A guidance package to aid this initiative was launched in 2016 by the UK government aptly named “Teacher Subject Specialism Training” (TSST), which focused primarily on maths and physics (Department for Education, 2016) but has since been withdrawn as of 2024 and handed over to the “National Centre for Excellence in the Teaching of Maths” (NCETM). To account for this retraining factor, we may assume a constant retraining rate $C > 0$ that occurs uniformly throughout the year, representative of teachers training inside and outside the academic year. This then gives a new periodic birthrate function:

$$B_2(t) := \sin\left(2\pi\left(t + \frac{1}{2}\right)\right) + 1 + C$$

Extending this further, we can use the ever-increasing hiring targets proposed by the Department for Education each year to account for the increased number of students in the secondary education system (Department for Education, 2024b). For simplicity, we may assume that the targets increase linearly each year^{III} at some rate D , giving the final, birthrate function:

$$B_3(t) := \sin\left(2\pi\left(t + \frac{1}{2}\right)\right) + 1 + C + Dt.$$

The three proposed functions are summarised in Figure 8.

Although no data on the exact number of teachers retraining into maths within England has been publicised, leaving us unable to confidently find a value for C , there are many reports from across the country which support the claim that this is not uncommon (BBC,

^{III}Which we see is a viable assumption from Figure 9

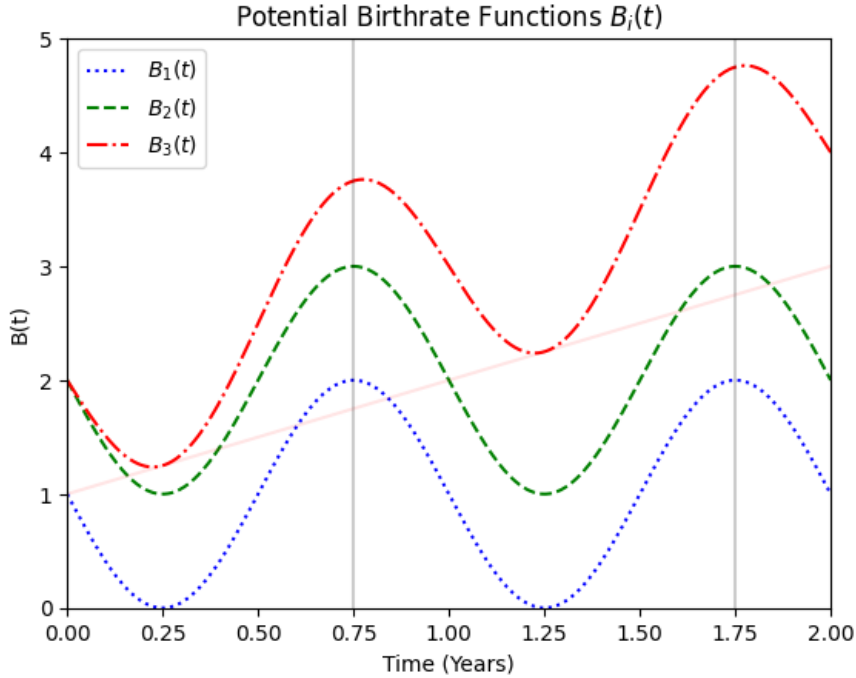


Figure 8: Plots of the proposed birthrate functions $B_i(t)$ for $i = 1, 2, 3$. The two vertical black lines show the peaks of each curve in the month of September, and the straight red line shows the linear relation $Dt + C$ upon which $B_3(t)$ builds.

2024). Despite this, we may use data from the UK Government on “Postgraduate Initial Teacher Training Targets” (Department for Education, 2024b) and the “Initial Teacher Training Census” (Department for Education, 2024a) to obtain a linear estimate for the gradient D . We can do this by plotting the data points from each dataset and taking a linear interpolant of the data similar to that of Section 3.1, this can be seen in Figure 9.

From Figure 9, we find that the hiring target’s line of best fit may be approximated by the linear relation:

$$f(t) = 171.5t - 344144.80$$

meaning the government, on average, aim to hire 171 additional teachers throughout England than they hired in the previous year. In contrast to this, looking at the actual hiring data, which may be approximated by the linear relation:

$$g(t) = -95.54t + 195358.16$$

we see that the government are missing their targets quite substantially, possibly as a consequence of the COVID-19 pandemic, and instead hiring fewer teachers each year than in the year prior. Despite this, we may conclude that D can be expressed as:

$$D := \frac{N + 171}{N} \approx 1$$

for large N .

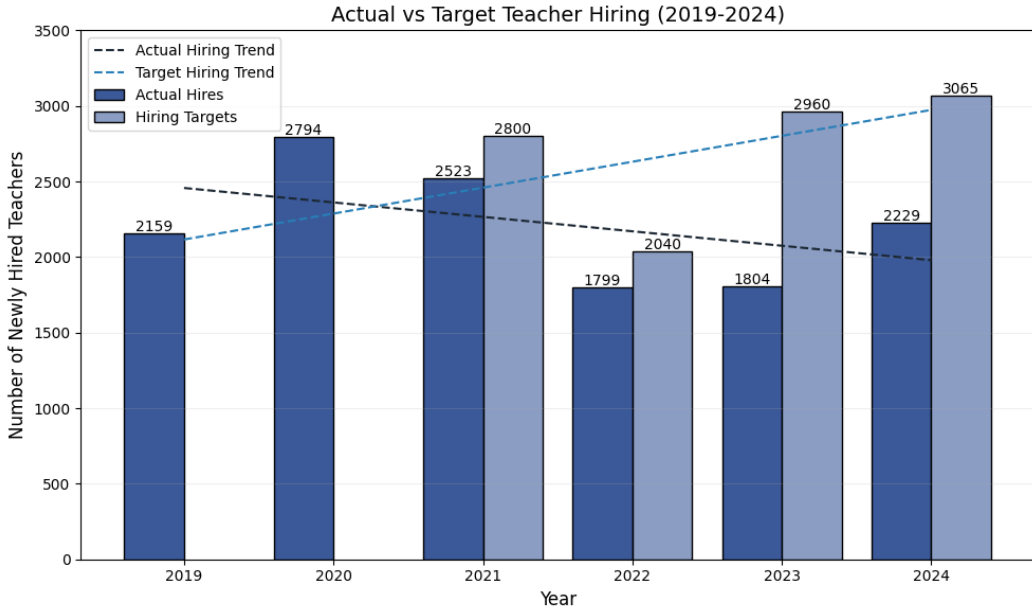


Figure 9: Plot of the actual hiring data against the target hiring data for maths teachers in England from 2019 to 2024. The left bars show actual hires and the right show the target for each year. A linear interpolant is used to find line of best fit for each, plotted as the dashed lines above and below. Note that the data post 2022 may be pouted as a response to the COVID-19 pandemic. (Department for Education, 2024b)

3.3 Variable Support $K(\mathbf{x})$

In the original model, we use the parameter $K \in [-1, 1]$ to account for the general support teachers receive within the education system; whilst this greatly simplifies the analysis of the problem, it grossly abstracts the complex factors at play in measuring the mental well-being of an individual. In this section, we provide alternative ways to model this parameter as a time-dependent function that might better fit the real-world context of our problem.

Following a similar pattern to Section 3.1, we could begin by extending our model to account for population-specific support parameters K_i which account for the unique challenges faced by each group (Education and Training Foundation, 2021). Doing this creates 3 new parameters K_0, K_1 and K_2 which could then be tuned with respect to studies undertaken into the well-being of teachers at different stages of their career, which is beyond the scope of this project.

Developing this further, we may instead look to identify the key factors effecting an individual's general well-being and opinion of their job, with which we can then define a function which appropriately weights their contributions. A meta-analysis conducted in 2014 (Aloe *et al.*) highlighted the effect of student misbehaviour and its contribution to the three dimensions of burnout identified in teachers, those being: emotional exhaustion, reduced accomplishment and depersonalisation. Similarly, a further meta-analysis conducted in 2021 (Madigan and Kim) looked at the same three dimensions, along with

job satisfaction, and to what extent each contributed towards predicting whether an individual had intentions to quit their job. The analysis found their relative weights to be: emotional exhaustion 36.46%, depersonalisation 16.60%, reduced accomplishment 9.80% and job satisfaction 37.14%. A number of surveys have also been carried out throughout the country identifying that 41% of teachers describe their workload as “unmanageable”, 37% describe their workload as “only just manageable” while only 1% say that their workload is manageable “all the time” (National Education Union, 2024). Similarly, University College London (UCL, 2023) highlights that a report by the Department for Education quotes professional development as a key contributor to job satisfaction, within 98% of individuals undertaking some CPD in 2022. Finally, studies have shown that higher salaries and targeted financial rewards can enhance teacher retention, particularly in challenging school environments (Education Endowment Foundation, 2023). Conversely, substantial pay gaps between teaching and non-teaching professions in certain regions correlate with higher teacher attrition rates (Education Policy Institute, 2021) suggesting a balance in local labour markets could help to improve retention.

With these key contributors having been identified from the literature (burnout, job satisfaction, student misbehaviour, workload, professional development opportunities and salary expectations), we can look to define functions which encapsulate the dynamics of each factor before collating them all in a weighted sum function whose outputs $K(\mathbf{x}) \in [-1, 1]$, as per our original problem constraints, for a vector $\mathbf{x} \in \mathbb{R}$ which takes in numerous inputs discussed throughout the following sections.

Financial Incentives:

As outlined in Chapter 1, as of 2025, there are bursary and early career payment schemes in place which total to a maximum of £75,000 for qualifying candidates. This money is paid across the PGCE year (Get Into Teaching and Teaching Maths Scholars, 2024) and the first year of teaching (Department for Education, 2024c), encouraging a “take the money and run” approach to ECTs. Modelling this as some function $f_1(t; \lambda)$, which shows the effect financial incentives have on an individual’s willingness to remain in teaching. We naturally choose an exponential decay with rate $\lambda > 0$, representing the rate at which the financial incentive depletes an individual’s motivation, and normalised to 1 at $t = 0$:

$$f_1(t; \lambda) := e^{-\lambda t}$$

If instead, the £75,000 was distributed throughout the first few years of teaching, we could model the effect of financial incentives by a decaying sinusoidal function of the form:

$$f_2(t; A) := \left(\frac{\cos(\frac{t\pi}{4})}{1 + At} \right)^2$$

where the period of the cosine function has been arbitrarily rescaled to 4 years so that payments are spread across a sufficient number of years to ensure individuals remain in teaching for many years whilst staying regular enough to have a moderate effect on motivation. In order to have our sinusoidal function $f_2(t)$ accurately approximate the

original function $f_1(t; \lambda)$, we can choose parameters λ and A such that their integrals coincide on a given interval $[0, T]$. To do this, we fix $T = 30$, simulating a teaching career of 30 years as we hope to maintain teachers long into the C_2 population, and fixing their integrals:

$$\int_0^T f_1(t; \lambda) dt = \int_0^T f_2(t; A) dt = 7.5$$

where the 7.5 simulates the possible £75,000. Evaluating their integrals numerically, using a root finding algorithm to find the location where their integral difference is small, we obtain the parameter values:

$$\lambda = 0.13069, \quad A = 29.878 \quad (5.S.F)$$

with difference in integrals being $8.9459 \cdot 10^{-5}$

The plots of these functions can be seen in Figure 10.

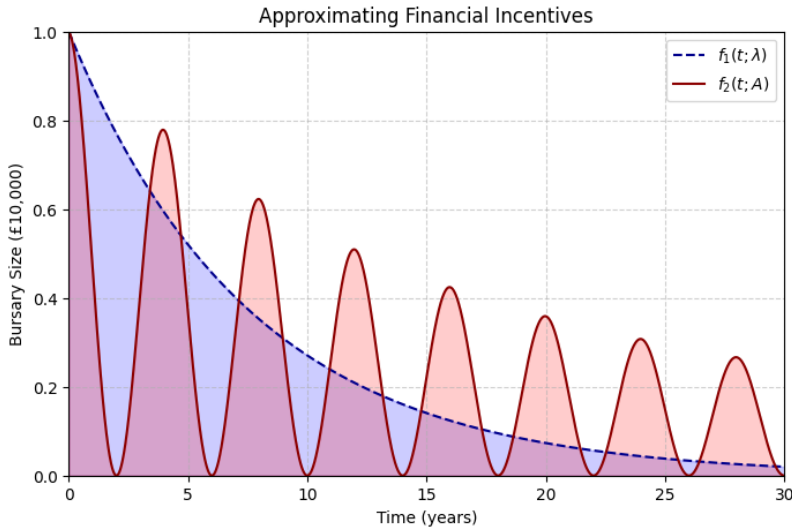


Figure 10: Plot of the proposed financial incentive functions $f_1(t; \lambda)$ and $f_2(t; A)$ with $\lambda = 0.13069$ and $A = 29.878$ chosen to ensure near equivalence of their integrals (i.e red and blue shaded areas are of same size).

Burnout:

To model how the effects of burnout contribute to support and well-being within our model, we note that the dynamics of burnout may be characterised by the existence of some critical value where a drastic change happens, akin to a **bifurcation point**. In this context, a bifurcation in burnout occurs when the factors identified by Madigan and Kim (2021) become so detrimental to an individual's job that they are unable to work effectively and risk entering the vulnerable category. Representing this behaviour mathematically can be done through an activation function such as the translated and scaled sigmoid

function:

$$B(x; b) := \frac{2}{1 + e^{bx}} - 1 \in (-1, 1)$$

for some $x \in \mathbb{R}$ and $b \in \mathbb{R}^+$.

Here, x quantifies the factors previously identified that lead to burnout, and $b > 0$ is a measure of support provided by the school to their staff. The characteristic S-curve of the sigmoid function defines an interval about the origin where slight permutations in x , through support or further overwhelm, lead to drastic changes in $B(x; \lambda)$; but beyond this, changes in x have insignificant impacts on $B(x; \lambda)$. Ideally, we aim to reduce x so that burnout is low in teachers, contributing to a positive total effect. Intuitively, this models the ineffectiveness of support systems for extreme cases where individuals may already be well-supported or too far gone so that small interventions will have little to no impact, supporting the work of Iancu *et al.* (2018) who highlight the importance of early intervention in combatting burnout.

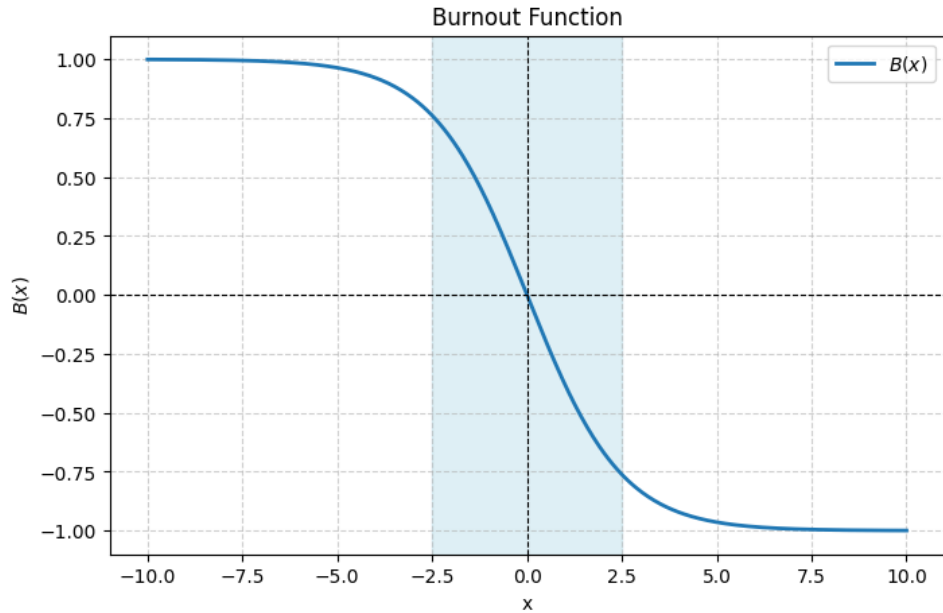


Figure 11: An example plot of $B(x; b)$ for $b = 0.8$ showing the sigmoid function's shape. The highlighted area showcases the region of sensitivity with respect to small perturbations in x .

Professional Development Opportunities:

Using the work of Dreyfus and Dreyfus (1988), who characterised the learning experience with sigmoid curves, representing an initially slow learning process followed by a phase of rapid improvement before plateauing at “mastery”, we may apply this to the effectiveness of CPD throughout an individual’s career. With the goal of CPD being “to improve teaching quality and keep teachers in the profession through effective CPD” (Cordingley *et al.*, 2015), we may assume that the sigmoid function proposed in Section 3.3 (or equivalently Figure 11) may also be used here up to a change in parameter b .

Job Satisfaction:

To create a simple function which models how an individual's job satisfaction varies over time, we can use the work of Dobrow Riza, Ganzach, & Liu (2018) who found that satisfaction decreases with respect to time whilst remaining in a single career, but increases when swapping career. Using this in our model, we may model job satisfaction through exponential decay, translated and scaled to fit $(-1, 1]$ as follows:

$$j(t; \mu) := e^{-\mu t + \ln(2)} - 1 \in (-1, 1]$$

for some scalar $\mu \in \mathbb{R}^+$ representing the rate at which an individual loses interest in their career.

Notably, this function, shown in Figure 12, starts at 1, and approaches -1 as $t \rightarrow \infty$, representing the growing dissatisfaction which comes with working the same job for many years. The parameter μ could be tuned by survey data and an exponential model fit, but is left arbitrary for the purposes of this project.



Figure 12: Plot of a translated exponential decay function $j(x)$ with notable features $j(0) = 1$ and $\lim_{t \rightarrow \infty} j(t) = -1$

Workload:

A 2016 report by the Education Policy Institute (EPI, 2016) found that teachers worked an average of 48.2 hours a week, which was nearly 20% more than other professions, rising to 52.4 hours a week in 2023 (Schools Week, 2023). With teachers sinking additional hours each week into marking assessments or preparing lessons, workload has consistently been a major issue in disputes surrounding the profession, and hence a critical factor in the well-being of an individual. Despite being a complex item to model, we may simplify the

analysis to a linear function:

$$w(x) := 1 - \frac{T(x)}{T_{\max}} \in [(-\infty, 1]$$

where $x \in \mathbb{R}$ measures the quantity of work and $T(x) \in \mathbb{R}^+$ the respective amount of time completing that work. We then define T_{\max} to be the maximum amount of time each week an individual is expected to work so that when $T(x) > T_{\max}$ we have $w(x) < 0$, representing the negative effect on mental well-being as work becomes overwhelming, seeping into other aspects of a teacher's life. Using this function, we see that $w(x)$ is theoretically unbounded from below, to solve this problem we simply assert a minimum of -1 by taking:

$$W(x) := \max\{w(x), -1\} \quad \forall x \in \mathbb{R}.$$

The function $w(x)$ is assumed to be some polynomial in x , which expresses the relationship between work and time to complete, Figure 13 shows plots for degree 1 and 2 polynomials. For polynomials of degree 2 or less, $W(x)$ can be constructed in a way so that it decays to -1 where it remains fixed for all time. But for higher order polynomials there is the more likely possibility that $w(x) > -1$ for more than one interval (see Figure 14) and so we assume that $w(x)$ is of degree 2 or less to avoid this.

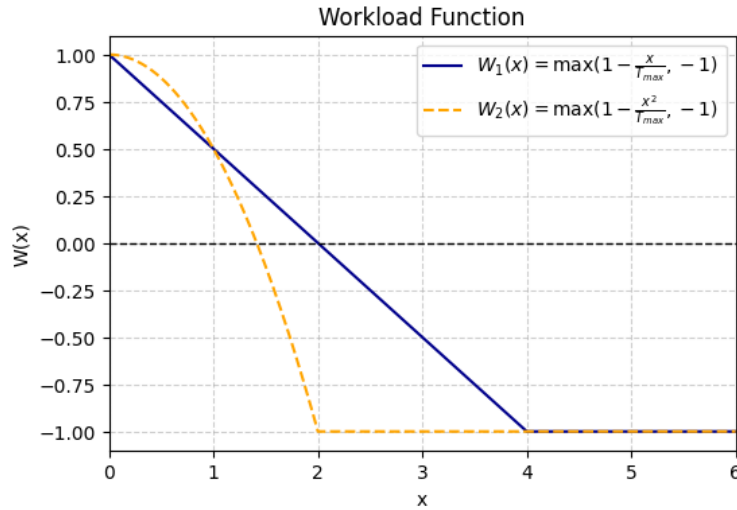


Figure 13: Two possible plots for the workload function $W(x)$, the first uses a linear function, $w_1(x) = x$, and the second a quadratic, $w_2(x) = x^2$. Both decay to -1 where the maximum assertion caps their value.

Student Misbehaviour:

Identified throughout the literature as a key factor contributing to emotional exhaustion, with Tsouloupas *et al.* stating “teacher perceptions of student misbehaviour is directly and positively associated with emotional exhaustion” (Tsouloupas *et al.*, 2010). Furthermore, the meta-analysis conducted by Aloe *et al.* (2014) highlights the strong association between classroom management and teacher attrition, emphasising the importance of its

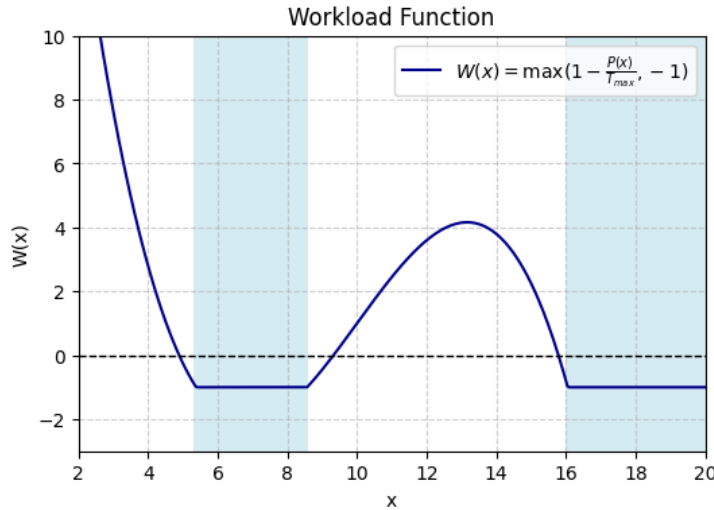


Figure 14: A degenerate case of $W(x)$ where we use a degree 3 polynomial $P(X) = 0.1x^3 - 3x^2 + 27x - 70$ which falls beneath -1 for two distinct intervals, shaded in blue, which is unrealistic for this context.

inclusion in the modelling of teacher well-being within our model system. To do this, we may intuitively assume that when student misbehaviour is low, the effect it has on the teacher is also low; but as more time is spent dealing with incidents, a greater deal of stress is put on the teacher. Formulating this mathematically, we may look to make use of the normal or Gaussian distribution:

$$M(t; s) := 2e^{\frac{t^2}{s}} - 1 \in (-1, 1]$$

where $t \in \mathbb{R}^+$ is the amount of time spent dealing with incidents and $S \in \mathbb{R}^+$ is some measure of support received by the teacher from the school itself in regards to behaviour management. Plotted in Figure 15, this shows the brief interval where classroom management is within the teachers control, followed by a gradual decay to the point of harming the teacher's well-being.

Weighted Sum $K(\mathbf{x})$:

With the above functions defined, we can construct our final support function $K(\mathbf{x})$ which depends on some vector $\mathbf{x} \in \mathbb{R}^n$ of all of the above parameters. The term $K(\mathbf{x})$ should be some weighted average which takes in the outputs of the contributing functions and scales them by some $w_i \in (0, 1)$ such that their sum is 1:

$$w_B + w_F + w_P + w_J + w_W + w_S = 1$$

where, from left to right, each w_i represents to the respective weighting of: burnout, financial incentives, professional development, job satisfaction, workload and student misbehaviour. Combing this with the function outputs themselves, we obtain the final function:

$$K(\mathbf{x}) := w_B \cdot B(t) + w_F \cdot F(t) + w_P \cdot P(t) + w_J \cdot J(t) + w_W \cdot W(\mathbf{x}) + w_S \cdot S(\mathbf{x}) \in (-1, 1).$$

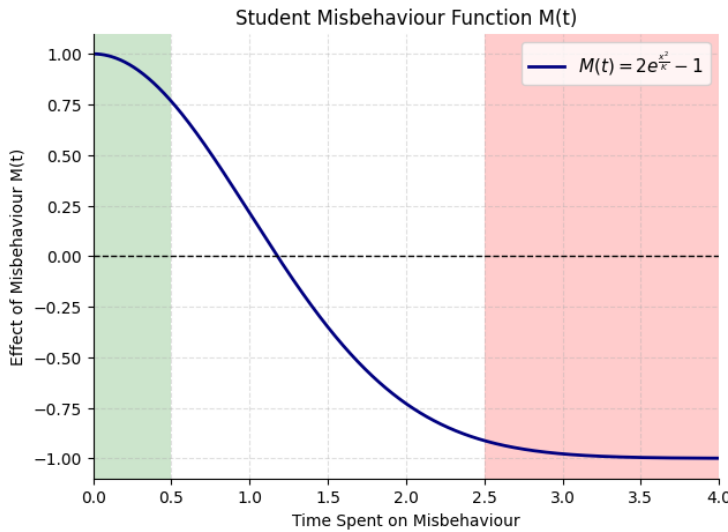


Figure 15: An example plot for the effects of student misbehaviour on a teacher’s well-being. The shaded area on the left shows the initial, manageable region where only a small portion of time is spent managing students. The shaded area on the right shows the point where student misbehaviour is too difficult to control and reaches its maximum detrimental effect on a teacher’s well-being.

4 Opinion Polling in Teacher Recruitment

Despite their similarities, the population dynamics involved in career modelling may differ from epidemiological models as they are more heavily influenced by individual decisions and collective behaviours throughout the wider community. Traditional models of disease spread, which our model has been inspired by, often assume uniform transition rates between classes, yet the decisions made throughout an individual’s career, particularly in the case of choosing whether to switch careers, are inherently strategic and largely shaped by social influence (Xu, 2021). This chapter extends the original model proposed in Section 2.1 by incorporating game-theoretic techniques, inspired by Reluga, Bauch and Galvani (2006), to better capture the complexities of the movement between the previously defined comfortable, vulnerable, and removed states.

4.1 Game Theoretic Model Description

The paper by Reluga, Bauch and Galvani (2006) explores the interplay between individual decision-making and community-level behaviour using a game-theoretic approach to voluntary vaccination. They extend the classic SIR model proposed by Kermack and McKendrick (1927) to account for the strategic decisions individuals undertake when deciding to vaccinate or not, introducing two key frameworks for modelling decision-making dynamics:

- **Best-Response Dynamics:** Individuals act to maximise the personal utility of a

choice based on perceived risks and rewards, leading to a Nash equilibrium where no one can improve their situation.

- **Imitation Dynamics:** Individuals adapt their behaviour based on the perceived actions of others in the system, leading to socially reinforced strategies.

A key conclusion made through their investigations is that Nash equilibria often lead to suboptimal vaccine coverage due to an insufficient personal risk-reward payout; whilst community-optimal behaviour required much higher vaccine uptake that was only possible if imitation dynamics dominated the decision-making process.

These frameworks provide direct motivation for the modification of the basic model proposed in Section 2.1 to account for the strategic career decisions made within our model that may be influenced by personal factors such as salary, workload and stress (best-response dynamics) as well as accounting for community factors that come from social interactions and media outlets (imitation dynamics).

We begin by formulating our new game-theoretic model, this time condensing our system by considering a single comfortable and vulnerable class for simplicity – although this could instead be presented as an investigation into a single target career group from the model in Section 2.1. Using the standard SIR model as a starting point, we obtain the following:

$$\frac{dC}{dt} = -\beta CV + \gamma V \quad (3a)$$

$$\frac{dV}{dt} = \beta CV - \gamma V - \delta V \quad (3b)$$

$$\frac{dR}{dt} = \delta V \quad (3c)$$

where:

- β represents the rate at which comfortable teachers become vulnerable by mixing populations within a school.
- γ represents the recovery from vulnerable to comfortable as support is provided by the school.
- δ represents the rate at which vulnerable teachers leave the profession.

Note that this system does not include a birth rate term, as we are only considering the decision-making mechanics within a single academic year for simplicity. This allows us to ignore any new entrants and simply focus on the internal dynamics.

Whilst rigid parameter values allow for broad analysis to be undertaken, this model fails to account for the strategic nature of career decisions and the multifaceted dependencies on more human factors such as workload, burnout, or salary expectations which contribute to the overall utility of a decision.

4.2 Incorporating Best-Response Dynamics

An individual's transition between the three populations within our system may be viewed as a strategic choice influenced by personal payoffs which individuals aim to maximise by considering the risk and reward of swapping state. For example, an individual may move from comfortable to vulnerable after deciding they should put less effort into their work as they believe they are not being paid enough, or an individual may enter the removed class if they believe it is feasible that they could earn more and be happier in another profession. To formalise this process, we require payoff functions that quantify the benefit or loss for each change of state.

Suppose that the payoff function $P_X : \mathbb{R}^n \rightarrow \mathbb{R}$, represents the benefit or loss of entering population X depends on n -many factors such as salary, workload, burnout etc. We then use a binary logit choice model to evaluate the probability that an individual in population X enters population Y by:

$$\alpha := \frac{e^{P_Y}}{e^{P_Y} + e^{P_X}} \in (0, 1)$$

which could then be substituted into the SIR model to more accurately quantify the transition rates based on the key factors influencing the underlying dynamics of the model.

In the context of our model, we can quantify the payoff functions by considering the key factors that Madigan and Kim (2021) identified as influencing teacher attrition, those being salary, workload and burnout, which is itself a combined measure of emotional exhaustion, depersonalisation, reduced accomplishment and job satisfaction. For simplicity, we define the following linear payoff functions, though higher-order functions may also be implemented, simply by adding positive attributes and subtracting negative ones:

$$\begin{aligned} P_C &:= S - W \\ P_V &:= S - (W + B) \\ P_R &:= U - I \end{aligned}$$

where:

- S represents salary benefits,
- W represents workload stress,
- B represents general burnout,
- U represents the general benefits of a new career,
- I represents the financial insecurity of changing career.

To avoid any terms disproportionately dominating the payoff functions, we require each term to be of equivalent order, e.g $S, W, B, U, I \sim \mathcal{O}(10^{-1})$ such that each is in the interval

$[-1, 1]$ to mimic being non-dimensionalised. In this setting, P_C and P_V differ only by the addition of a burnout term, B , which accounts for the additional stress of feeling uncertain in their career; whilst P_R balances the benefits that may come with a new job, U , such as increased pay or job satisfaction, with the initial financial insecurity I that comes with finding a new job such as a brief period of unemployment.

With the relevant payoffs defined, we can then redefine the transition rates β and δ as follows:

$$\beta := \frac{e^{P_V}}{e^{P_V} + e^{P_C}} \quad \text{and} \quad \delta := \frac{e^{P_R}}{e^{P_R} + e^{P_V}}.$$

Note that the recovery rate γ is not a strategic choice that an individual makes, but the result of some input from an external force, e.g. support from the school, hence it is not modelled by a binomial logit choice like β and δ . Greater analysis could be undertaken into the dynamics of school-level support for teachers, and is discussed in Section 6.4, but is beyond the scope of this project.

4.3 Incorporating Imitation Dynamics

In addition to individual strategic decision-making, the perceived behaviour of one's peers also heavily influences the decisions an individual makes, particularly if a decision leads to a change in the relationships that affect their daily life (Xu, 2024). The peer pressure an individual feels to conform with the rest of the population emerges through imitation dynamics with the inclusion of an additional weighted term that represents the community's influence on a particular decision. These terms are designed to capture the idea that an individual's likelihood of transitioning between states increases when they observe a higher proportion of their peers in their state; and can be defined by:

$$\eta X(f_X - X)$$

where:

- η is the imitation rate, quantifying how influenced an individual is by their peers,
- f_X represents the observed number of individuals in state X (where X is C , V or R) from the perspective of other individuals in the system so that movement between states is partially driven by crowd behaviour.

This imitation term is similar to an internal competition term commonly seen throughout predator-prey dynamics, which is proportional to the difference between perceived and actual populations in each state. We see that when $f_X > X$ there is a movement into class X , whilst the reverse happens if $f_X < X$. This suggests that increasing f_X , through a positive media campaign for example, will push individuals into the X class with diminishing returns as X consequently increases, reducing the imitation term's effect in time. Incorporating these terms into our previous model from Section 4.2, we obtain the following extended model which accounts for both individual and community decision

making dynamics:

$$\frac{dC}{dt} = -\beta CV + \gamma V + \eta C(f_C - C) \quad (4a)$$

$$\frac{dV}{dt} = \beta CV - \gamma V - \delta V + \eta V(f_V - V) \quad (4b)$$

$$\frac{dR}{dt} = \delta V + \eta R(f_R - R). \quad (4c)$$

This allows us to easily investigate the dynamics of the system with and without the community influence by setting $\eta = 0$ or $\eta > 0$. To then ensure that the output of our system remains within the interval $[0, 1]$ we non-dimensionalise as in Section 2.2, once again rescaling the populations by $N = C + V + R$ and rescaling time by $T = 1$ as before. This gives:

$$\frac{dC}{dt} = -\frac{\beta CV}{N} + \gamma V + \frac{\eta C}{N} (f_C - C) \quad (5a)$$

$$\frac{dV}{dt} = \frac{\beta CV}{N} - \gamma V - \delta V + \frac{\eta V}{N} (f_V - V) \quad (5b)$$

$$\frac{dR}{dt} = \delta V + \frac{\eta R}{N} (f_R - R) \quad (5c)$$

Essentially rescaling $\beta \rightarrow \frac{\beta}{N}$ and $\eta \rightarrow \frac{\eta}{N}$, leaving the remaining parameters unchanged.

4.4 Steady State Analysis

As in Section 2.4, we now look to investigate the analytic forms of our steady states. As, for the purpose of this investigation, we are only interested in the working populations within our new game-theoretic model, we will ignore the removed category R and focus only on steady states (C^*, V^*) . Finding the zeros of Equations (5), we are able to identify the following four cases:

- Case 1:** $(0, 0)$
- Case 2:** $(f_C, 0)$
- Case 3 & 4:** $\left(\frac{\pm\sqrt{X} + Y}{Z}, \frac{\pm\beta\sqrt{X} + W}{\eta Z} \right)$

where:

$$\begin{aligned}
X &= (\delta N - \eta f_V)^2 \beta^2 + 4\eta^2 f_C \left[\left(\gamma + \frac{\delta}{2} \right) N - \frac{\eta f_V}{2} \right] \beta \\
&\quad - 4\eta^2 \left[\gamma(\gamma + \delta)N^2 - \eta\gamma f_V N - \frac{\eta^2 f_C^2}{4} \right] \\
Y &= [-\eta f_V + (\delta + 2\gamma)N]\beta + \eta^2 f_C \\
Z &= 2(\beta^2 + \eta^2) \\
W &= [2\eta f_V + \beta f_C - 2N(\delta + \gamma)]\eta^2 + (\eta f_V - N\delta)\beta^2.
\end{aligned}$$

To ensure each case is biologically realistic, we once again require that both $C^*, V^* \geq 0$. However, unlike in Section 2.4 we have a non-negativity condition on all parameters, leading to a much simpler analysis. Despite this simplification, we are left without a parameter, such as K previously, with respect to which we may define the necessary conditions for existence, as any parameter is just as important as the others in this system.

Case 1: We immediately see that this case is trivially biologically realistic as it depends on no parameter values, hence remaining constant at the origin no matter how one varies the system and exists for all choices of parameters. Although this is realistic, it is unfeasible in the context of our problem as we would have no working teachers in the entire population due to the lack of birthrate.

Case 2: As in Case 1, we immediately conclude that $V^* = 0$ is, again, trivially biologically realistic. Looking to $C^* = f_C$, we note that $f_C \geq 0$ by our non-negativity assumption, and hence $C^* \geq 0$, thus this steady state always exists.

Cases 3 & 4: For non-negativity to hold in this case, we first note that $Z \geq 0$ and so we are left only with proving non-negativity for the numerator of each steady state. For both cases, we require $X \geq 0$ to avoid having complex solutions, to find such a case, we note that:

$$X = X(\beta) = A\beta^2 + B\beta + C$$

where

$$\begin{aligned}
A &= (\delta N - \eta f_V)^2 \\
B &= 4\eta^2 f_C \left[\left(\gamma + \frac{\delta}{2} \right) N - \frac{\eta f_V}{2} \right] \\
C &= -4\eta^2 \left[\gamma(\gamma + \delta)N^2 - \eta\gamma f_V N - \frac{\eta^2 f_C^2}{4} \right].
\end{aligned}$$

Thus, we see that $X > 0$ when $\beta \notin [X_-, X_+]$ where X_-, X_+ are roots of $X(\beta)$. In this case, for $C^* \geq 0$ we hence require:

$$\pm\sqrt{X} + Y \geq 0$$

Splitting this into the positive and negative cases we find:

$$\begin{aligned}-\sqrt{X} + Y > 0 &\implies \sqrt{X} < Y \\ \sqrt{X} + Y > 0 &\implies \sqrt{X} > -Y\end{aligned}$$

thus we may combine both expressions to give $\sqrt{X} < |Y|$. Finding expressions for the above in terms of the model parameters would present a lengthy condition on an arbitrarily selected parameter, and so has been left as above for simplicity.

Moving onto V^* , we follow a similar method, noting once again that the denominator is positive from the non-negativity of our parameters – leaving us with the task of proving non-negativity for the numerator:

$$\pm\beta\sqrt{X} + W \geq 0$$

We may split these into the positive and negative cases to obtain the two inequalities:

$$\begin{aligned}-\beta\sqrt{X} + W > 0 &\implies \beta\sqrt{X} < W \\ \beta\sqrt{X} + W > 0 &\implies \beta\sqrt{X} > -W\end{aligned}$$

where, just as before, the two expressions combine to give $\sqrt{X} < |\frac{W}{\beta}|$. Hence we conclude that when $X > 0$, which is to say $\beta \notin [X_-, X_+]$, we have biological realism for some choice of parameters.

4.5 Stability Analysis

In contrast to the previous system discussed in Section 2.1, our new game-theoretic system is much simpler to analyse, in terms of steady state stability, with it being a coupled pair of equations when the removed category R is ignored as our main focus lies with the comfortable and vulnerable populations C and V respectively. Analysing the stability thus equates to looking at the traces and determinants of the Jacobian matrix evaluated at each steady state and comparing to Figure 5.28 from Strogatz's book "Nonlinear Dynamics and Chaos" (1994, p. 138) which builds on the work of Routh (1877) and Hurwitz (1895), collating their theory on the classification of steady states into what is more commonly recognised today as the "Routh-Hurwitz Diagram" shown in Figure 16.

By constructing our Jacobian matrix J of partial derivatives, we find:

$$J = \begin{bmatrix} -\frac{1}{N}[\beta V + \eta(2C - f_C)] & -\frac{\beta C}{N} + \gamma \\ \frac{\beta V}{N} & -\frac{1}{N}[(2V - f_V)\eta + (\delta + \gamma)N - \beta C] \end{bmatrix}$$

which can then be evaluated at each of the four steady states (C^*, V^*) identified in Section 4.4 so that we might use their traces and determinants to classify their shape and stability.

Case 1: $(0, 0)$

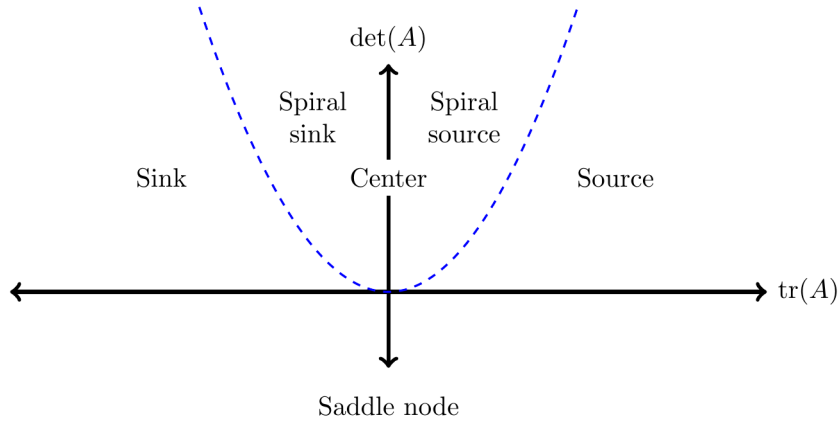


Figure 16: A plot showing the different shaped nodes and their stability as the trace and determinant of their Jacobian matrix varies (Zobitz, n.d.).

In the case of the trivial steady state $(0, 0)$, we obtain the Jacobian:

$$J_{(0,0)} = \begin{bmatrix} \frac{\eta f_C}{N} & \gamma \\ 0 & \frac{\eta f_V}{N} - \delta - \gamma \end{bmatrix}$$

which gives:

$$\text{tr} = \frac{\eta}{N}(f_C + f_V) - (\delta + \gamma) \quad \Delta = \frac{\eta f_C(\eta f_V - (\delta + \gamma)N)}{N^2}$$

By the Routh-Hurwitz stability criterion we, or equivalently Figure 16, we require $\Delta > 0 > \text{tr}$ for $(0, 0)$ to be considered stable. Therefore:

$$\text{tr} = \frac{\eta}{N}(f_C + f_V) - (\delta + \gamma) < 0 \implies (f_C + f_V)\eta < (\delta + \gamma)N$$

$$\Delta = \frac{\eta f_C(\eta f_V - (\delta + \gamma)N)}{N^2} > 0 \implies \eta f_C f_V > (\delta + \gamma)N$$

which combine to give:

$$f_C + f_V < f_C f_V$$

otherwise $(0, 0)$ is unstable. We may also consider the shape of the steady state by considering where in the (tr, Δ) plane the steady state lies by evaluating the quantity $\text{tr}^2 - 4\Delta$ and its relation to 0:

$$\text{tr}^2 - 4\Delta = \frac{((f_C - f_V)\eta + N(\delta + \gamma))^2}{N^2} \geq 0$$

which means $(0,0)$ is either a stable node when $\text{tr}^2 - 4\Delta > 0$ or a stable star node when $\text{tr}^2 - 4\Delta = 0$ which can be classified as follows:

$$\text{tr}^2 - 4\Delta \begin{cases} = 0, & (f_V - f_C)\eta = (\delta + \gamma)N \\ > 0, & \text{otherwise.} \end{cases}$$

Case 2: $(f_C, 0)$ Evaluating the Jacobian matrix at $(f_C, 0)$ gives:

$$J_{(f_C, 0)} = \begin{bmatrix} -\frac{\eta f_C}{N} & -\frac{\beta f_C}{N} + \gamma \\ 0 & \frac{\beta f_C + \eta f_V}{N} - (\delta + \gamma) \end{bmatrix}$$

which gives:

$$tr = \frac{(f_C + f_V)\beta - \eta f_C}{N} - (\delta + \gamma) \quad \text{and} \quad \Delta = \frac{\eta f_C ((\delta + \gamma)N - (\beta f_C + \eta f_V))}{N^2}$$

Once again, we can evaluate the cases for which these produce stable steady states by the Routh-Hurwitz stability criterion, which requires:

$$\begin{aligned} tr = \frac{(f_C + f_V)\beta - \eta f_C}{N} - (\delta + \gamma) < 0 &\implies (f_C + f_V)\beta - \eta f_C < (\delta + \gamma)N \\ \Delta = \frac{\eta f_C ((\delta + \gamma)N - (\beta f_C + \eta f_V))}{N^2} > 0 &\implies (\delta + \gamma)N > \beta f_C + \eta f_V. \end{aligned}$$

We may then once again classify the form of these stable steady states by considering the quantity $tr^2 - 4\Delta$ and its relation to 0:

$$tr^2 - 4\Delta = \frac{((\delta + \gamma)N - (f_C + f_V)\eta - \beta f_C)^2}{N^2} \geq 0$$

which gives rise to the same situations as in Case 1, stable node for inequality and stable star node for equality, which occur when:

$$tr^2 - 4\Delta \begin{cases} = 0, & (\delta + \gamma)N = (f_C + f_V)\eta + \beta f_C \\ > 0, & \text{otherwise} \end{cases}$$

Cases 3 & 4: $\left(\frac{\pm\sqrt{X+Y}}{Z}, \frac{\pm\beta\sqrt{X+W}}{\eta Z}\right)$

Rather than explicitly evaluating the Jacobian for the steady states in Cases 3 and 4, we work generally with the traces and determinants and substitute in at the end, this yields:

$$\begin{aligned} tr &= \frac{-2\eta(C + V) + (f_C + f_V)\eta - (\delta + \gamma)N + (C - V)\beta}{N} \\ \Delta &= \Delta(\eta) = \frac{A\eta^2 + B\eta + C}{N^2} \end{aligned}$$

where

$$\begin{aligned} A &= 4 \left(C - \frac{f_C}{2} \right) \left(V - \frac{f_V}{2} \right) \\ B &= 2(\delta + \gamma) \left(C - \frac{f_C}{2} \right) N - 2\beta \left[C \left(C - \frac{f_C}{2} \right) - V \left(V - \frac{f_V}{2} \right) \right] \\ C &= NV\beta\delta. \end{aligned}$$

Thus to satisfy the Routh-Hurwitz criterion we require:

$$tr = \frac{-2\eta(C + V) + (f_C + f_V)\eta - (\delta + \gamma)N + (C - V)\beta}{N} < 0$$

$$\implies (f_C + f_V)\eta + C\beta < (\delta + \gamma)N + (\beta + 2\eta)V + 2\eta C$$

and for $\Delta > 0$ we require $\eta \in (\eta^-, \eta^+)$ or $(-\infty, \eta^-) \cup (\eta^+, \infty)$, depending on the sign of A , where η^- and η^+ are roots of the polynomial $\Delta(\eta)$ which have the form:

$$\eta^\pm = \frac{-B \pm \sqrt{B^2 - 4AC}}{2A}$$

However, the discriminant of the above varies in sign as each parameter is changed, which is summarised in Table 2.

$C - \frac{f_C}{2}$	$V - \frac{f_V}{2}$	A	$B^2 - 4AC$
+	+	+	±
+	-	-	+
-	+	-	+
-	-	+	±

Table 2: The signs of A and $B^2 - 4AC$ based on the sign of the first two columns.

To that ensure $\Delta > 0$, we consider see that when both quantities have different parity, so that $B^2 - 4AC > 0$ holds based on signs alone, we guarantee that $\eta^\pm \in \mathbb{R}$. Since $A < 0$ in this situation, for $\Delta > 0$ we require $\eta \in (-\infty, \eta^-) \cup (\eta^+, \infty)$ but since $\eta > 0$ by construction, this reduces to ensuring at least $\eta^+ > 0$ through a choice of parameters to ensure B small.

Similarly, for the remaining two cases in the table above where $A > 0$, we see that considering the signs is not enough to ensure $B^2 - 4AC > 0$ and so we require a careful choice of parameters so that this holds to guarantee $\eta \in \mathbb{R}$. Just as before, for $\Delta > 0$ we now require $\eta \in (\eta^-, \eta^+)$ with the additional assumption that some subinterval is strictly positive which can be found by once again requiring at least $\eta^+ > 0$.

With the steady states, and their respective stabilities, of the game-theoretic model constructed by Equations (5) explored, we now look to generalise the two proposed models to an arbitrary workplace so that the work carried out in this project may be more widely applicable throughout workplace dynamics.

5 Adapting to Careers Beyond Teaching

The dynamics of the career pipeline in many professions share structural similarities with the flow of individuals through the SIR model adapted for the purposes of this project. While previous chapters have focused specifically on the teaching profession, this

chapter aims to generalise the core ideas used throughout our research to a wider range of professional contexts.

Depending on the specific structure of the career one chooses to apply this methodology, there is merit to following either of the models previously suggested. Those being the time progression model from Chapter 2 which accounts for steady progression through roles as an individual spends more time within a career, or the short-time model from Chapter 4 which focuses on the community aspect and local dynamics with respect to a single role. We will begin by developing general frameworks for the analysis of each, then propose suggestions for collecting data to inform parameter choices for each, and conclude by providing a series of steps in order to analyse each framework.

5.1 Career Progression Framework:

For the first model, a generalisation of the work carried out in Chapter 2, we define the system for $M + 1$ sequential roles obtained through tenure:

$$\frac{dC_0}{dt} = B - \alpha_0 C_0 + KC_0 V_0 \quad \frac{dV_0}{dt} = -\alpha_0 V_0 - KC_0 V_0 - \beta V_0 \quad (6a)$$

$$\frac{dC_i}{dt} = \alpha_{i-1} C_{i-1} - \alpha_i C_i + KC_i V_i \quad \frac{dV_i}{dt} = \alpha_{i-1} V_{i-1} - \alpha_i V_i - KC_i V_i - \beta V_i \quad (6b)$$

$$\frac{dC_M}{dt} = \alpha_{M-1} C_{M-1} + KC_M V_M - \beta C_M \quad \frac{dV_M}{dt} = \alpha_{M-1} V_{M-1} - KC_M V_M - \beta V_M \quad (6c)$$

$$\frac{dR}{dt} = \beta \left(C_M + \sum_{i=0}^M V_i \right) \quad (6d)$$

for $i = 1, 2, \dots, M - 1$ and where:

- B is the birthrate of the system, representing newly hired workers who begin in the 0th role. This can be found and tuned by examining the hiring data of a company/profession and averaging the annual hires for simplicity.
- $\alpha_i \in [0, 1]$ are the rates at which individuals transition between classes with respect to time found by inverting the length of each class, that is, if C_i lasts for $x > 0$ years, $\alpha_i = \frac{1}{x}$.
- $\beta \in [0, 1]$ is the rate of attrition, representing the rate at which people in the vulnerable state leave the profession by quitting or retiring. This can be found and tuned by investigating the attrition data of a company/profession and averaging the annual attrition rates for simplicity.
- $K \in [-1, 1]$ is the rate at which individuals move between comfortable and vulnerable states, representing the support an individual receives at work. This can be investigated by conducting regular support surveys amongst employees and evaluating the effectiveness of resources available to manage workload and stress.

As before, this system models two simultaneous populations, comfortable and vulnerable, with exchange occurring between the two when support is inadequate, $K < 0$. Though the system above provides a general purpose model for investigating career progression, there are a number of modifications that could be made depending on workplace contexts; some of these may include:

- B_i , introducing a birthrate into each C_i equation may be more realistic if a company/profession recruits for roles throughout their company rather than just entry-level positions represented by C_0 and V_0 .
- $C_{i,j}$, collate multiple roles into the same tier C_i , which may represent salary thresholds or seniority positions to group analysis more appropriately.
- $\tilde{\alpha}_i X_i$ terms in the j^{th} equation, for $j > i + 1$ representing employees from the i^{th} role progressing straight to the j^{th} role and skipping intermediate positions as a fast track route due to performance or previous experience.

Once necessary modifications have been made to the system, one should follow the steps below to carry out an investigation into the populations and their steady state values in order to inform relevant policy change:

1. Non-Dimensionalise the model by considering $\tilde{X}_i := \frac{X_i}{N}$.
2. Carry out numerical investigations to validate model structure.
3. Identify steady state solutions by considering the vectors

$$\mathbf{X}^* := (C_0^*, C_1^*, \dots, C_M^*, V_0^*, \dots, V_M^*) \quad \text{such that} \quad \frac{d\mathbf{X}_i}{dt}|_{\mathbf{X}^*} = 0.$$

4. Evaluate the stability and shape of each steady state by considering the Jacobian matrix $J := \left[\frac{d}{d\tilde{X}_j} \left(\frac{d\tilde{X}_i}{dt} \right) \right]_{ij}$ evaluated at each steady state and the sign of their eigenvalues.
5. Identify the populations that need maximising and/or minimising, and the parameter changes required to achieve each of these.
6. Construct policy changes informed by steady state analysis which leads to the desired changes.

5.2 Local Decision-Driven Framework

For the second model, a generalisation of the game-theoretic model outlined in Chapter 4 which takes place on a short time-scale such that birthrate is no considered, we utilise

the same equations as before:

$$\frac{dC}{dt} = -\beta CV + \gamma V + \eta C(f_C - C) \quad (7a)$$

$$\frac{dV}{dt} = \beta CV - \gamma V - \delta V + \eta V(f_V - V) \quad (7b)$$

$$\frac{dR}{dt} = \delta V + \eta R(f_R - R). \quad (7c)$$

where:

- $\beta \in [0, 1]$ is the rate at which comfortable employees enter the vulnerable class. This may be found and tuned by conducting regular surveys with employees to keep track of well-being and job satisfaction.
- $\gamma \in [0, 1]$ is the rate at which vulnerable employees naturally recover back into the comfortable class after company intervention and could be found through exit interviews or regular well-being checks.
- $\delta \in [0, 1]$ is the rate of attrition throughout the system, representing the rate at which employees quit or retire. This can be tuned by looking at the attrition data of a company/profession.
- $\eta \in [0, 1]$ is the imitation rate of a profession, this quantifies to what extent an individual's decision-making may be influenced by their peers. This could be found through regular internal surveys to track the sense of community within the workplace.
- $f_X \in [0, 1]$ is the perceived number of individuals in class X (that being C, V or R) and represents how the wider population views the split of individuals between a given set of classes. This may again be found through internal surveys into the state of the company/profession.

Similar to the methods explored in Chapter 4, we may replace any of the parameters above, excluding f_X with a logit choice model:

$$\alpha := \frac{e^{P_Y}}{e^{P_Y} + e^{P_X}} \in (0, 1)$$

where P_X and P_Y represent the pay off attached to entering populations X and Y respectively. These payoff functions may then be defined as a weighted sum of N -many positive, a_i^+ , and negative, a_i^- , attributes related to entering each population:

$$P_X := \sum_{i=1}^N (a_i^+ - a_i^-) \quad \text{where } a_i^+, a_i^- > 0.$$

As in Section 5.1, whilst the system above provides a general purpose model for decision-based career movement, specific workplace models may require further modification to better grasp the dynamics at play. Examples of such modification may include:

- $\eta X_i(f_{X_i}^e - X_i)$: introduces the effect of an external perception $f_{X_i}^e$ of a given career. This may be a contributing factor for more public-facing or careers where a level of accolade or criticism is pushed onto employees from the general public driven by widespread biases.
- ρC : includes an additional removal term from the comfortable class into the removed class to simulate career progression, such as a promotion into a new class beyond the role that the 3-population system focuses.

Once necessary modifications have been made to the system in order to better fit the context, an investigation into the steady states of the above system can be undertaken using the method below to formulate relevant policy changes:

1. Non-Dimensionalise the model by considering $\tilde{X}_i := \frac{X_i}{N}$.
2. Carry out numerical investigations to validate model structure.
3. Identify steady state solutions by considering the vectors $\mathbf{X}^* := (C^*, V^*)$ such that $\frac{dX_i}{dt} \Big|_{\mathbf{X}^*} = 0$.
4. Evaluate the stability and shape of each steady state by considering the Jacobian matrix $J := \left[\frac{d}{dX_j} \left(\frac{dX_i}{dt} \right) \right]_{ij}$ evaluated at each steady state, using Figure 16 to classify stability.
5. Identify the parameter changes that must occur to maximise C^* whilst minimising V^* .
6. Construct policy changes informed by steady state analysis which lead to the desired changes.

6 Conclusions and Future Work

6.1 Summary of Findings

We began this project by establishing the context of the mathematics teacher crisis in England (Section 1.1) noting the large sums of money, up to £75,000, available to new applicants juxtaposed with the governments repeated failure to meet their own targets each year. With that in mind, we defined our problem by choosing to focus on the severe recruitment and retention challenges faced by the Department for Education, highlighted in the workforce census data we have used throughout to tune our work. Using this data, we identified the worryingly high attrition rates within the first 10 years of teaching, and used this to motivate the construction of our compartmental model, choosing to take a nuanced dynamical systems approach towards the issue, in the hopes of identifying key areas for efforts to be directed, with quantitative data from our model system to support our conclusions, in order to better supply the nation with a supply of passionate teachers ready to educate the next generation.

Building on the work of Kermack and McKendrick (1927), we adapted the traditional SIR model to account for the unique dynamics present in each of the three distinct career stages, narrowing our focus to the exploration of recruitment, attrition, and the effects of support structures on the teacher population. By creating a transfer diagram of our system (see Figure 1) we were able to construct the basis of our model in Equations (1) which was later non-dimensionalised in Equations (2) to better understand the outputs of our equations. Before conducting any analytic work, we undertook a handful of numerical investigations in Section 2.3 to validate the model's behaviour and justify the choice of parameter labels. Content with the model framework, we analytically investigated the system to obtain expressions for the steady states rigorously finding conditions for their existence in Section 2.4, concluding that there are a possible 3 biologically feasible steady states depending on the value of $K \in [-1, 1]$, these being Cases 1, 2 and 5. We then used the Routh-Hurwitz Stability Criterion to prove that each steady state has at least one stable direction, but cannot be considered locally stable due to a partition of the possible values of K leading to the constant existence of at least one unstable direction when $K \neq 0$ (see the table at the end of Section ??), though in the event that $K = 0$, we have that all steady states are locally asymptotically stable.

Acknowledging the limitations of our original model from Equations (2), in Chapter 3 we explored the possibility of replacing the fixed parameters β, B and K with functions instead, focusing on theoretical implementation over any formal steady state analysis or simulation. Government census data was used to tune the attrition rate β , first to class specific rates, followed by a time-dependent function $\beta(t)$ as a cubic polynomial interpolant from the same data (see Figure 7). The birthrate B was also replaced by a number of sinusoidal functions that accounted for the cyclic hiring structure of the academic year (see Figure 8), the retraining of teachers to specialise in mathematics as a secondary subject, and the ever increasing government hiring targets. The support parameter K was developed to include numerous psychological and financial factors, each with a brief functional description of their own, in order to better capture the complex nature of the parameter (see Figures 10, 11, 12, 13, 14, 15). These extensions of the basic model aim to better capture the nuanced dynamics involved in the teaching profession as well as better approximating the trends in data used to tune our model and provide a basis for any future work which may be conducted on this specific case.

We then presented an alternate perspective by extending the work of Reluga, Bauch, and Galvani (2006) on the game-theoretic dynamics of vaccine uptake to our employment context by considering both individual and collective decision-making processes within one's career. Starting with the basic SIR model, we introduced best-response dynamics in Section 4.2 which represents the maximisation of personal utility based on workload, salary, and burnout. Followed by imitation dynamics in Section 4.3, which capture the influence of peer behaviours in communal environments. We then followed a similar approach to the analysis of our basic model, by conducting steady state analysis on the pair of relevant equations using the Routh-Hurwitz Diagram in Figure 16 to classify the shape and stability of each steady state in Section 4.5.

Following this, two alternate frameworks were proposed in Chapter 5 that acknowledge the similarities in dynamics across professions. The first was a career progression model,

much like that of Chapter 2, while the second was a local decision-driven model, like that of Chapter 4. Both frameworks were proposed in general terms and provided guidance on how individuals could define the necessary parameters and obtain data to tune them. A general methodology used throughout this project was also provided for those who wish to conduct their own investigation using this project as a starting point.

6.2 Limitations and Assumptions

Throughout this project, a number of assumptions have been made in order to reduce the complexity of our system and the attached calculations. Whilst the more computationally impactful assumptions have been explored in Chapter 3, there are a number of assumptions made implicitly about the dynamics as a result of our choice of model. Although the underlying dynamics remain relatively unaffected without these, a number of human factors have been ignored or generalised in favour of simplicity, not capturing the multifaceted human elements at play.

The use of ordinary differential equations assumes continuous, deterministic transitions between the different classes of teachers explored throughout this project. Although this allows for relatively simple construction and analysis of model systems, it neglects to acknowledge any stochastic variation that may be present as a result of random fluctuations in human behaviour. By assuming that all individuals express identical behaviour, the system is too well-behaved in comparison to real data, which is rarely smooth like our equations predict. The introduction of stochastic variation could help to capture the randomness of unpredictable events, such as local policy changes or sudden shifts in school environments, better representing the reality of the teaching profession whilst creating a more resilient model for capturing the effects of variable support levels. In particular, including a random movement between the three classes, representing some drastic external change in an individual's life, could lead to non-zero vulnerable steady states even in the case of $K > 0$.

Similarly, the model explored in Chapter 4 presumes that individuals within the system make career decisions solely on the basis of maximising payoffs derived from factors such as salary, workload, and burnout. In assuming this, we have ignored the complex human behaviours that may drive these decisions such as personal values, social pressures, or health concerns. Despite the payoff functions providing a convenient analytical foundation for this project, they fail to acknowledge the inherent randomness present among humans that greatly affect such choices, limiting the appropriateness of such terms within our model.

Another assumption made by the choice of a continuous modelling framework is that the transition between classes are immediate, not accounting for the real-word limitations that would likely lead to delays in movement between populations. It is more realistic, instead, to assume that individuals leave at convenient times in the academic calendar, such as the end of each term or semester, rather than continuously throughout the entire year. To account for this, there is merit in choosing a discrete system determined by equations of the form $x_{n+1} = f(x_n, x_{n-1})$ to better model these delays by considering

previous iterations of each population.

Finally, the interpolation of functions based on data including the last five years (2020-2025) may be compromised by abnormal data from the COVID-19 pandemic and its aftermath. The pandemic altered typical classroom dynamics, pushing teaching online and piling onto the already unmanageable workload of teachers to provide an equally holistic learning experience despite the circumstances. During this period, Figure 9 clearly shows a significant reduction in newly hired teachers, in line with the Office of National Statistics' report (ONS, 2021) which found a notable fall in employment and vacancies during the height of the pandemic. Consequently, the tuning of functions based on this data may be negatively skewed as a result of the struggling job market. Despite this, with the pandemic having greatly altered many workplace dynamics, encouraging many remote working options across multiple industries, it is important to still consider this data going forward as the education sector begins to rebuild from these numbers before returning to previous trends.

6.3 Policy Implications

With the three key attributes contributing to the steady state values of our system being the support K , recruitment B , and retention β , we now look to identify potential initiatives and policy proposals which could help to increase each parameter accordingly. Whilst the explicit needs of recruitment and retention vary throughout the cases explored in the previous section, it is clear that support is the most significant factor at play, highlighted by Case 1 of our analysis in Section 2.4 which leads to the zero vulnerable population situation for positive or insignificantly negative K . For that reason, we look first at how teachers may be better supported through a variety of new initiatives.

Enhancing Teacher Support Through Integrated Initiatives

Financial incentives are a cornerstone for improving teacher support, with 84% of teachers in 2023 stating pay levels as a cause for stress in England and Wales (NEU, 2024). Whilst there already exist a number of bursaries and scholarships available to those undergoing initial teacher training courses, totalling up to £75,000, as explored in Section 3, which often leads to exploitation of the system. To combat this, as recommended by the NFER (2021), the UK government should redesign the current early career payments schemes by widening eligibility and increasing “payment generosity”. As we previously showed in Figure 10, this could be done by better distributing funds through the first few years of an individual’s career to maintain motivation, or by increasing the total amount and introducing a “Retention Premium” for teachers who consistently demonstrate high performance and commitment throughout their career. On average, even if the total amount was increased, this could lead to a wider saving from the government as individuals may leave the profession before receiving the total sum allocated to them. This money could then be recycled into the system to fund further bursaries such as the Teacher Subject Specialism Training (TSST) (Department for Education, 2015) which had previously hoped

to attract non-specialist teachers into critical subjects such as maths, physics, chemistry and computing (NFER, 2021).

Continuing Professional Development (CPD) and mentoring schemes play a critical role in bolstering support and personal achievement among teachers. Research has shown that well-designed CPD programs can help to improve classroom practices and boost overall job satisfaction and personal achievement (Cordingley *et al.*, 2015). Sutton (2021) found that good CPD involved many members of the department from all levels to foster a healthier working community, included interactive practice-based skills development with room for reflection on individual beliefs and values, and focussed on the needs of both staff and students with the goal of providing a well-rounded educational experience. Embedding these opportunities into the school calendar, coupled with mentorship schemes to further facilitate personal growth, ensures teachers have access to learning opportunities which have been tied to reducing burnout and improving staff retention (Sutton, 2021). A possible scheme to help support this initiative could involve a “Professional Growth Fund” for each member of staff, which allows time and resources to be spent on CPD and formal qualifications to help develop the skill sets of teachers more generally.

Studies by the National Education Union (NEU, 2024) highlight the excessive workload teachers face each day with 95% of teachers in England and Wales stating their work-life balance as a source of stress, and only 21% of individuals agreeing that their workload is manageable most or all of the time. The teaching career is prolific for the intense workload, so changes must be made to offload non-teaching tasks and provide better administrative support to teaching staff. Some schools in the private sector have dedicated staff in each department to support teachers in such activities, an idea which could be implemented into the public sector with great effect. Additionally, inspiration could be taken from the Finnish education system in giving teachers more autonomy in the planning of lessons and school management which has been praised for its positive effect on job satisfaction and overall well-being (Sahlberg, 2015).

Together, these initiatives could work towards the development of a comprehensive support strategy, far beyond the scope of this project, which could help to significantly improve the well-being of teachers in the UK in the hopes of making the teaching profession more attractive with its competitive pay, integrated CPD and work-life balance.

Recruitment Strategies for the Education Sector

With the UK government repeatedly missing their ever-increasing hiring targets for new teachers each year, see Figure 9, recruitment drives are clearly failing. Many university graduates are initially deterred by the relatively modest starting salaries of £29,000-£35,000 and limited career progression when compared to careers in finance or technology (EPI, 2021). Although the UK’s education sector has a clearly structured pay-scale system (NASUWT, 2024) which allows for incremental increases as educators gain experience and take on greater responsibilities, research by the NEU suggests that these increases fail to appropriately compensate individuals for the workload, stress and added responsibilities that come with the job (NEU 2024). This disparity between industry and teaching

salary expectations contribute significantly to recruitment challenges, specifically in secondary mathematics (EPI, 2021) and must be addressed through policy reform, salary increases and performance-related incentives to better align with competing careers which are currently much more appealing to applicants. Countries such as Luxembourg have some of the highest teaching salaries in the Organisation for Economic Co-operation and Development (OCED, 2023) with a starting salary of around €77,000 (roughly £66,000), making it an especially well-respected and valued career which lead to more passionate educators and competitive employment markets.

Studies have also shown that the perceived status of teaching, including society wide undervaluation and general lack of respect from both students and peers beyond the career, heavily influence graduates' decisions (Ingersoll, 2001), with 26% of teachers across the OCED stating that they felt their profession is valued in society (OCED, 2023). To combat this harmful idea, government initiatives should be launched by groups such as Teach First or Get Into Teaching which highlight the critical role that teachers play in shaping future generations and acknowledge their hard work on a wider societal level. To ensure that teacher's themselves feel empowered at work, a greater emphasis should be put on CPD, allowing individuals to develop their skills and work on qualifications such as National Professional Qualifications (Government of the United Kingdom, 2024) to further their career progression.

Initiatives to Reduce Teacher Attrition

With government census data showing that the education sector has one of the highest attrition rates across the UK labour market, teacher attrition is a persistent issue which must be addressed if the government are to meet their goal of providing a competitive secondary school education. Throughout the career, the highest attrition rates lie in the ECT years of an individual, suggesting a greater need for support during the early years of a teacher's career. Sutton (2021) suggests extending the structured mentoring that ECTs receive beyond the initial two-year induction period and to include a greater level of guidance to help teachers navigate the increasing responsibilities that come with the role. This support could come in the form of mentorship, CPD, or regular well-being checks led by leadership teams during performance reviews to cultivate a culture where well-being is prioritised. Such checks have been repeatedly proposed by the NFER (2022) who claim it would lessen the effects of burnout and by proxy attrition.

Another proposal by the NFER (2022) is the idea of mid-career CPD sabbaticals, allowing educators the opportunity to dedicate 1-2 terms to professional development, research, or training without the pressures of teaching. The proposal hopes to rejuvenate teachers by encouraging them to reflect on their passion to teach and educational practices so they might return with a fresh mind and motivation to continue within the career. In 2018, the Department for Education explored the feasibility of sabbatical schemes, quoting them as a possible solution to teacher attrition (Department for Education, 2018). Similarly, flexible working policies have also been suggested by the NEU (2024) as a possible solution to attrition by promoting healthy work-life balances in high-need subjects such as mathematics and, more generally, in the case of accommodating teachers with caring

responsibilities.

A study by the Department for Education (2023a) found that 75% of teachers reported spending excessive amounts of time on administrative work, focussing mostly on data entry, paperwork and communication. These clerical duties often contribute to burnout and job dissatisfaction due to the misalignment with an educator's core duties. Instead, this work should be delegated to administrative staff to enable teachers the opportunity to concentrate solely on their primary role of educating students in order to reduce attrition rates. The Department for Education's "Workload Reduction Taskforce" aims to combat this by decreasing working hours by 5 per week within the next few years (Department for Education, 2023a), and NASUWT repeatedly advocate for the hiring of more administrative staff to offload the unnecessary work from classroom teachers.

6.4 Recommendations for Future Research

While the models and their respective analyses presented in this project hope to provide a foundational framework for exploring career dynamics, in the form of a case study on the Department for Education, several simplifications were necessary due to the project's time frame. Further research into this branch of mathematical modelling could aim to develop these ideas by introducing more detailed behavioural modelling or the addition of other population interactions. In strengthening the models proposed here, they may provide potential value as a practical tool used by policymakers to inform workforce reform to the benefit of teachers and students alike. What follows are suggestions for future work that build upon the ideas presented in this project.

An immediate extension to the original model would be to include additional entry terms into the system for teachers returning from career breaks or retraining to specialise in mathematics as a secondary subject, similar to that discussed in Section 3.2, allowing for an investigation into how these effect workforce sustainability. Alternatively, an entirely new category of returned and retrained teachers may be considered due to the unique dynamics present in their population, as these individuals may be more prone to burnout due to a lack of confidence in content delivery from inexperience or time away from the career. Going further, a measurement of teaching quality could be taken, to investigate the effect as a result of this "supplementary workforce" and an investigation could be undertaken on the link between retraining schemes and student performance.

Following a similar strain, the original model could be expanded to include the student population, modelling the interactions between students and teachers in relation to student misbehaviour and educational performance. This would allow for a systematic exploration of how teacher shortages may affect class sizes or overall student outcomes. Such a model could be used to identify feedback loops within the education system leading to positive or negative spirals that need to be addressed internally, by support staff, and institutionally, by the Department for Education. This could then be developed further to account for a limited supply of support resources managed by the school, modelling this as another population which contributes to the well-being of teachers and students alike. Together, the two ideas would allow for an investigation on how to best use the limited

available resources, ensuring teachers remain in the career comfortably, while ensuring students achieve high outcomes.

In alignment with systems such as Scotland's, which requires subject-specific qualifications in order to teach, the model system could be developed to look at the population of new graduates in England. Doing so would greatly develop the investigation into recruitment, by directly measuring the effectiveness on their target population, whilst tracking the proportion of fully qualified entrants over those with more general routes into teaching. Investigating how new graduates interact with the career would also further highlight any bottlenecks in recruitment pipelines as well as key attrition trends in exceptionally qualified individuals who may decide to change career for a more attractive salary beyond teaching. Combining this with some measure of educational quality or student outcome, as previously suggested, would then allow for the study of teaching quality in relation to previous qualifications, possibly pushing the Department for Education to take a similar stance to Scotland in order to up educational standards, with the additional opportunity to raise teacher salaries as a result of the increased entry requirements.

Appendices

A List of Acronyms

COVID-19: Coronavirus Disease 2019

CPD: Continuing Professional Development

ECT: Early Career Teacher

EEF: Education Endowment Foundation

EPI: Education Policy Institute

ITT: Initial Teacher Training

LTT: Long-Term Teacher

MEI: Mathematics in Education and Industry

MST: Mid-Stage teacher

NASUWT: National Association of Schoolmasters Union of Women Teachers

NCETM: National Centre for Excellence in the Teaching of Mathematics

NEU: National Education Union

NFER: National Foundation For Educational Research

OCED: Organisation for Economic Co-operation and Development

ONS: Office for National Statistics

OFQUAL: Office of Qualifications and Examinations Regulation

PGCE: Postgraduate Certificate in Education

SIR: Susceptible-Infectious-Recovered

TSST: Teacher Subject Specialism Training

UCL: University College London

B Section 2.3 Python Code

The following Python code was used in Section 2.3 to numerically approximate solutions to the proposed system of equations.

```
1 import numpy as np
2 import matplotlib.pyplot as plt
3 from scipy.integrate import solve_ivp
4
5 # Define parameters
6 #B = 0          # Birthrate (may be manually set)
7
8 K=0            # Support Parameter
9
10 a0 = 1/2       # Time Transition Rate (ECT - 2yrs)
11 a1 = 1/8       # Time Transition Rate (Mid Career - 8yrs)
12
13 b0 = 0.2       # ECT Attrition Rate
14 b1 = 0.2       # 5-10yr Attrition Rate
15 b2 = 0.2       # 10yr+ Attrition Rate
16 b3 = 0.2       # 10yr+ Retiring Rate
17
18 # Define Initial Populations for Each Class
19 initial_pop = [1/6, 1/6, 1/6, 1/6, 1/6, 1/6, 0] # Scaled to fit [0,1]
20
21 # Define the system of ODEs
22 def teacher_odes(t, y):
23     C0, C1, C2, V0, V1, V2, R = y                      # Populations
24     N = C0 + C1 + C2 + V0 + V1 + V2 + R                  # Total Population
25     # ODEs for each class
26
27     B = (b0*V0 + b1*V1 + b2*V2 + b3*C2)*N           # Fixed Population Birthrate
28
29     # "Comfortable" Equations
30     dC0_dt = B/N - a0*C0 + K*N*C0*V0
31     dC1_dt = a0*C0 - a1*C1 + K*N*C1*V1
32     dC2_dt = a1*C1 - b3*C2 + K*N*C2*V2
33
34     # "Vulnerable" Equations
35     dV0_dt = -a0*V0 - K*N*C0*V0 - b0*V0
36     dV1_dt = a0*V0 - K*N*C1*V1 - b1*V1 - a1*V1
37     dV2_dt = a1*V1 - K*N*C2*V2 - b2*V2
38
39     # Removed Equation
40     dR_dt = b0*V0 + b1*V1 + b2*V2 + b3*C2
41
42     return [dC0_dt, dC1_dt, dC2_dt, dV0_dt, dV1_dt, dV2_dt, dR_dt]
43
44 # Time span
45 TFinal = 40                                         # Set Long-Time Limit
46 t_span = (0, TFinal)                                 # Simulate from t=0 to TFinal
47 t_eval = np.linspace(*t_span, TFinal*100) # Evaluate Solutions
48
49 # Solve the ODEs
50 solution = solve_ivp(teacher_odes, t_span, initial_pop, t_eval=t_eval)
```

```

51
52 # Plotting
53 plt.figure(figsize=(10, 6))
54
55 line_colors = ['lightgreen', 'green', 'darkgreen', 'lightcoral', 'red',
56   'darkred', 'black']
57 line_styles = [':', '--', '-.', ':', '--', '-.', '-']
58 for i, label in enumerate(['C0', 'C1', 'C2', 'V0', 'V1', 'V2']):
59   # Add 'R' to Include Removed Class
60   plt.plot(solution.t, solution.y[i],
61     label=label, color=line_colors[i], linestyle=line_styles[i])
62 plt.xlabel('Time (Years)')
63 plt.ylabel('Population')
64 plt.title('Teacher Population Dynamics')
65
66 plt.grid(True, which='both', linestyle=':', linewidth=0.5, color='gray')
67 plt.xlim(0, TFinal)
68
69 plt.legend()
70 plt.show()

```

Bibliography

- [1] Aloe, A.M., Shisler, S., Norris, B.D., Nickerson, A.B. and Rinker, T.W. (2014) '*A multivariate meta-analysis of student misbehavior and teacher burnout*', *Educational Research Review*, 12, pp. 30–44. Available at: <https://www.sciencedirect.com/science/article/pii/S1747938X14000141> (Accessed: 10 October 2024).
- [2] BBC News (2024) '*Teacher shortages: PE staff retrain as maths teachers*'. Available at: <https://www.bbc.co.uk/news/education-68602435> (Accessed: 27 March 2025).
- [3] Chang, M.L. (2009) '*An appraisal perspective of teacher burnout: Examining the emotional work of teachers*', *Educational Psychology Review*, 21(3), pp. 193–218. doi: 10.1007/s10648-009-9106-y.
- [4] Cordingley, P., Higgins, S., Greany, T. and Buckler, N. (2015) *Developing Great Teaching: Lessons from the international reviews into effective professional development*. Teacher Development Trust. Available at: <https://tdtrust.org/wp-content/uploads/2015/10/DGT-Full-report.pdf> (Accessed: 30 March 2025).
- [5] Department for Education (2015) *Teacher subject specialism training courses*. Available at: <https://www.gov.uk/guidance/teacher-subject-specialism-training-courses> (Accessed: 30 March 2025).
- [6] Department for Education (2018) *Exploring the feasibility of a teacher sabbatical scheme*. Available at: <https://www.gov.uk/government/publications/teacher-sabbaticals-feasibility-study> (Accessed: 7 April 2025).
- [7] Department for Education (2023a) *Workload reduction taskforce*. Available at: <https://www.gov.uk/government/groups/workload-reduction-taskforce> (Accessed: 7 April 2025).
- [8] Department for Education. (2023b). *School Workforce Census 2023*. Available from: <https://www.gov.uk/government/collections/statistics-school-workforce> [Accessed 29 October 2024].
- [9] Department for Education (2024a) *Initial teacher training census: 2024 to 2025*. Available at: <https://explore-education-statistics.service.gov.uk/find-statistics/initial-teacher-training-census/2024-25> (Accessed: 27 March 2025).

- [10] Department for Education (2024b) *Postgraduate initial teacher training targets*. Available at: <https://explore-education-statistics.service.gov.uk/find-statistics/postgraduate-initial-teacher-training-targets> (Accessed: 27 March 2025).
- [11] Department for Education. (2024c). *Early career payments: Guidance for teachers and schools*. Available from: <https://www.gov.uk/guidance/early-career-payments-guidance-for-teachers-and-schools> [Accessed 2 January 2025].
- [12] Department for Education (n.d.) *Teacher subject specialism training courses*. Available at: <https://www.gov.uk/guidance/teacher-subject-specialism-training-courses> (Accessed: 29 March 2025).
- [13] Dobrow Riza, S., Ganzach, Y., & Liu, Y. (2018) 'Job satisfaction over time: A longitudinal study of the differential roles of age and tenure', *Journal of Management*, 44(7), pp. 2558–2579. Available at: https://www.researchgate.net/publication/276893636_Job_Satisfaction_over_Time_A_Longitudinal_Study_of_the_Differential_Roles_of_Age_and_Tenure (Accessed: 30 March 2025).
- [14] Dreyfus, H.L. and Dreyfus, S.E. (1988) *Mind over machine: the power of human intuition and expertise in the era of the computer*. 2nd paperback edn. New York: The Free Press, pp. 30–31.
- [15] Education and Training Foundation (2021) *Professional Standards: Supporting teachers and trainers throughout their career*. Available at: <https://www.etf-foundation.co.uk/professional-standards/teachers/career-stages/> (Accessed: 29 March 2025).
- [16] Education Policy Institute (2016) 'Teacher workload and professional development in England's secondary schools: insights from TALIS'. Available at: <https://epi.org.uk/publications-and-research/teacher-workload-professional-development-englands-secondary-schools-insights-talis/> (Accessed: 30 March 2025).
- [17] Education Policy Institute (2021) *Local Pay and Teacher Retention in England*. Available at: <https://epi.org.uk/publications-and-research/local-pay-and-teacher-retention-in-england/> (Accessed: 29 March 2025).
- [18] Get Into Teaching (2024) *How to fund your teacher training*. Available at: <https://getintoteaching.education.gov.uk/landing/how-to-fund-your-teacher-training> (Accessed: 18 April 2025).
- [19] Government of the United Kingdom (2024) *National professional qualification (NPQ) courses*. Available at: <https://www.gov.uk/guidance/national-professional-qualification-npq-courses> (Accessed: 7 April 2025).
- [20] Houpt, J.W. and Townsend, J.T. (2012) 'Statistical measures for workload capacity analysis', *Journal of Mathematical Psychology*, 56(5), pp. 341–355. doi:10.1016/j.jmp.2012.05.004.

- [21] Hurwitz, A. (1895) ‘Über die Bedingungen, unter welchen eine Gleichung nur Wurzeln mit negativen reellen Theilen besitzt’, *Mathematische Annalen*, 46, pp. 273–284.
- [22] Iancu, A. E., Rusu, A., Măroiu, C., Păcurar, R. and Maricuțoiu, L. P. (2018) ‘The effectiveness of interventions aimed at reducing teacher burnout: A meta-analysis’, *Educational Psychology Review*, 30(2), pp. 373–396. Available at: <https://eric.ed.gov/?id=EJ1179110> [Accessed: 29 March 2025].
- [23] Ingersoll, R. (2001) ‘Teacher turnover and teacher shortages: An organizational analysis’, *American Educational Research Journal*, 38(3), pp. 499–534. doi:10.3102/00028312038003499.
- [24] Kermack, W.O. and McKendrick, A.G., 1927. A contribution to the mathematical theory of epidemics. *Proceedings of the Royal Society of London. Series A, Containing Papers of a Mathematical and Physical Character*, 115(772), pp.700–721. Available at: <https://doi.org/10.1098/rspa.1927.0118> [Accessed 2 January 2025].
- [25] Kuddus, M.A., Meehan, M.T., Adekunle, A.I., White, L.J. and McBryde, E.S., 2019. *Mathematical analysis of a two-strain disease model with amplification*. arXiv preprint arXiv:1908.07837. Available at: <https://arxiv.org/abs/1908.07837> [Accessed 3 February 2025].
- [26] Madigan, D.J. and Kim, L.E. (2021) ‘Towards an understanding of teacher attrition: A meta-analysis of burnout, job satisfaction, and teachers’ intention to quit’, *Teaching and Teacher Education*, 105, 103425. Available at: <https://www.sciencedirect.com/science/article/pii/S0742051X21001499> [Accessed: 7 November 2024].
- [27] Mathematics in Education and Industry (MEI). (2024). *Recruiting, developing, and retaining the mathematics teaching workforce*. Available from: <https://mei.org.uk/app/uploads/2024/07/Maths-teacher-workforce-discussion-paper-July-2024.pdf> [Accessed 24 November 2024].
- [28] NASUWT (2024) *Pay scales England*. Available at: <https://www.nasuwt.org.uk/advice/pay-pensions/pay-scales/pay-scales-england.html> [Accessed: 7 April 2025].
- [29] NASUWT. (2019). *Teacher recruitment and retention: The challenges and the solutions*. Available from: <https://www.nasuwt.org.uk/static/uploaded/1ebdd1ff-aeac-422f-94fb7efa7df188c1.pdf> [Accessed 2 January 2025].
- [30] National Education Union (NEU) (2024) *State of Education: Workload and wellbeing*. Available at: <https://neu.org.uk/latest/press-releases/state-education-workload-and-wellbeing> [Accessed: 29 March 2025].
- [31] National Foundation for Educational Research NFER (2021) *The impact of training bursaries on teacher recruitment and retention*. Slough: National Foundation for Educational Research. Available at:

- https://www.nfer.ac.uk/media/bycg5uzk/the_impact_of_training_bursaries_on_teacher_recruitment_and_retention.pdf (Accessed: 6 April 2025).
- [32] National Foundation for Educational Research (NFER) (2022) *Teacher Labour Market in England Annual Report 2022*. Available at: <https://www.nfer.ac.uk/publications/teacher-labour-market-report-2022/> (Accessed: 7 April 2025).
- [33] National Foundation for Educational Research (NFER). (2024). *Teacher Labour Market in England: Annual Report 2024*. Available from: https://www.nfer.ac.uk/media/hqdglvra/teacher_labour_market_in_england_annual_report_2024.pdf [Accessed 29 October 2024].
- [34] OECD (2023) *Education at a Glance 2023: OECD Indicators*. Paris: OECD Publishing. Available at: https://www.oecd.org/en/publications/education-at-a-glance-2023_e13bef63-en.html (Accessed: 7 April 2025).
- [35] Office for National Statistics (2021) *Labour market overview, UK: April 2021*. Available at: <https://www.ons.gov.uk/employmentandlabourmarket/peopleinwork/employmentandemployeetypes/bulletins/uklabourmarket/april2021> (Accessed: 18 April 2025).
- [36] Ofqual. (2024). *GCSE Outcomes: Interactive Tool*. Available from: <https://analytics.ofqual.gov.uk/apps/GCSE/Outcomes/> [Accessed 2 January 2025].
- [37] Reluga, T.C., Bauch, C.T. and Galvani, A.P., 2006. Evolving public perceptions and stability in vaccine uptake. *Mathematical Biosciences*, 204(2), pp.185–198. Available at: <https://doi.org/10.1016/j.mbs.2006.08.015> [Accessed 2 January 2025].
- [38] Routh, E.J. (1877) *A treatise on the stability of a given state of motion: particularly steady motion*. London: Macmillan.
- [39] Sahlberg, P. (2015) *Finnish Lessons 2.0: What Can the World Learn from Educational Change in Finland?* New York: Teachers College Press.
- [40] Schools Week (2023) ‘Heads and teachers working longer despite workload push’. Available at: <https://schoolsweek.co.uk/heads-and-teachers-working-longer-despite-workload-push/> (Accessed: 29 March 2025).
- [41] Strogatz, S.H. (1994) *Nonlinear dynamics and chaos: with applications to physics, biology, chemistry, and engineering*. Reading, MA: Addison-Wesley. pp 138.
- [42] Sutton, A.L. (2021) *Exploring early career teachers' experiences of classroom behaviour they perceive as challenging and the continuous professional development that supports them*. PhD thesis. Available at: <https://www.proquest.com/dissertations-theses/exploring-early-career-teachers-experiences/docview/2685106536/se-2> (Accessed: 6 April 2025).

- [43] Tsouloupas, C.N., Carson, R.L., Matthews, R., Grawitch, M.J., & Barber, L.K. (2010). '*Exploring the association between teachers' perceived student misbehaviour and emotional exhaustion: the importance of teacher efficacy beliefs and emotion regulation*'. *Educational Psychology*, 30(2), pp. 173–189. Available at: <https://doi.org/10.1080/01443410903494460> (Accessed: 30 March 2025).
- [44] University College London (UCL) (2023) *Teachers and education leaders find workloads remain unacceptably high*. Available at: <https://www.ucl.ac.uk/ioe/news/2023/apr/teachers-and-education-leaders-find-workloads-remain-unacceptably-high> (Accessed: 29 March 2025).
- [45] Xu, H. (2021) *Career decision-making in an uncertain world: A dual-process framework*', *Current Psychology* 42, pp. 3978–3990. Available from: <https://link.springer.com/article/10.1007/s12144-021-01746-z> [Accessed 22 February 2025].
- [46] Zobitz, J. (n.d.) *Exploring Modeling with Data and Differential Equations Using R: Chapter 19 – Qualitative Stability Analysis*. Available at: <https://jmzobitz.github.io/ModelingWithR/stability-19.html> (Accessed: 15 April 2025).